

2025年7月6日至10日
Benismam Hall, Benikea Hotel, Jeju island
Asia/Seoul 时区

Nuclear cluster and hypernucleus production in intermediate-energy heavy-ion collisions

Zhao-Qing Feng (冯兆庆)

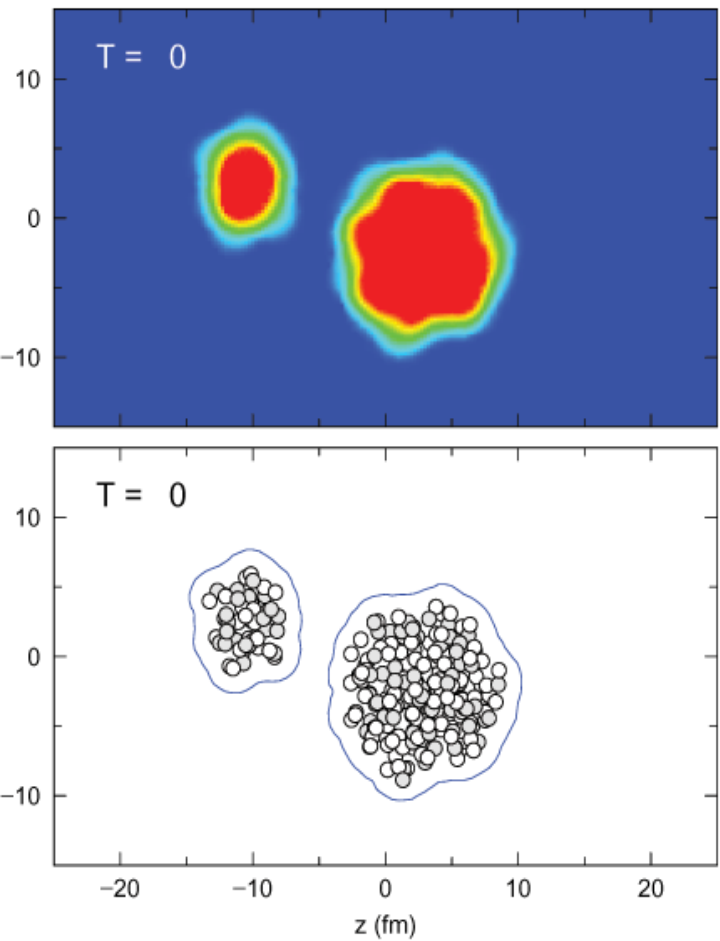
School of Physics and Optoelectronics, South China University of
Technology, Guangzhou

*Email: fengzhq@scut.edu.cn

Outline

- Cluster, hyperon and hypercluster production via heavy-ion collision for investigating neutron-star matter properties
- LQMD transport model
- Hyperon-nucleon interaction in dense nuclear matter via HICs
- Fragmentation reaction and hyperfragment production in HICs
- Summary and perspective

^{56}Fe 800 MeV/nucleon on ^{208}Pb



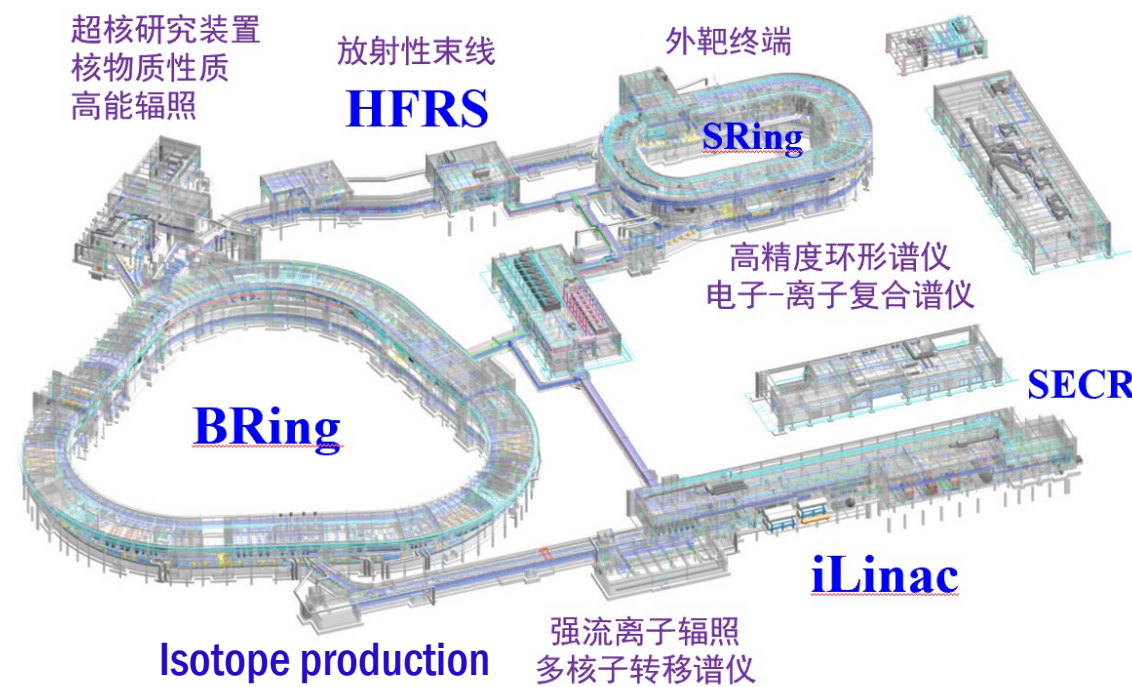
强流重离子加速器-HIAF



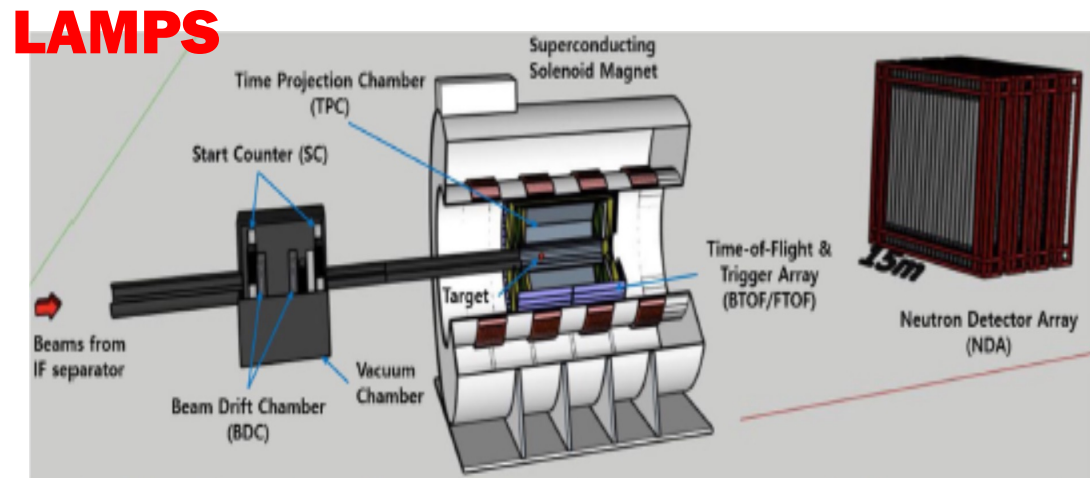
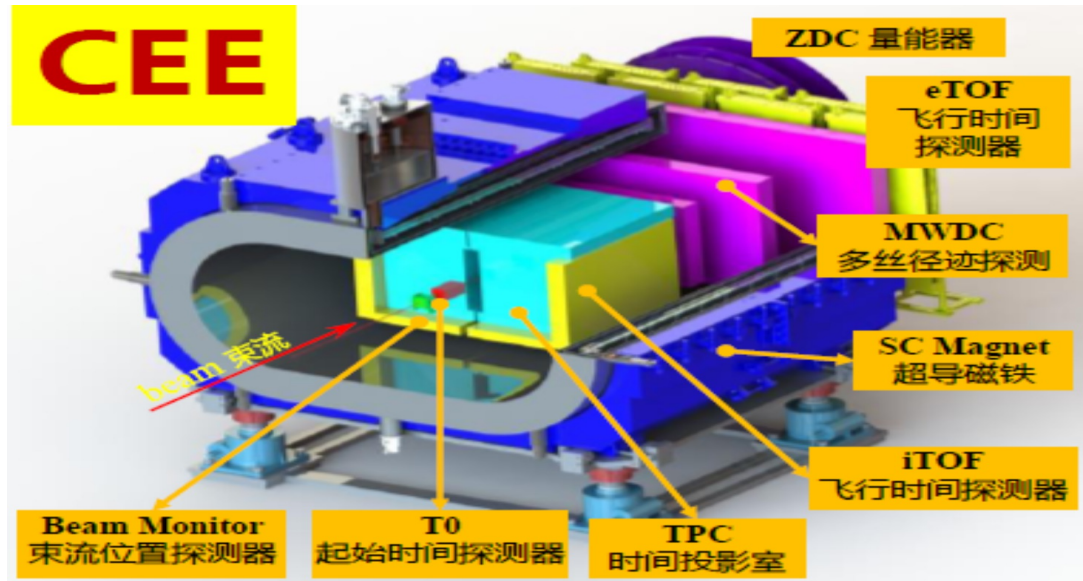
口 科学目标

集成离子超导直线加速器和环形同步加速器最先进的技术，建造一台束流指标先进、多学科用途的重离子科学综合研究装置—“强流重离子加速器研究装置”（HIAF），为核物理和核天体物理基础研究、原子物理、重离子束应用研究提供国际领先水平的实验平台。基于HIAF，打造在国际上有重大影响的重离子科学研究中心

总体方案：强流超导直线、快循环同步环、多实验终端结合



Korea-China cooperation for rare isotope physics

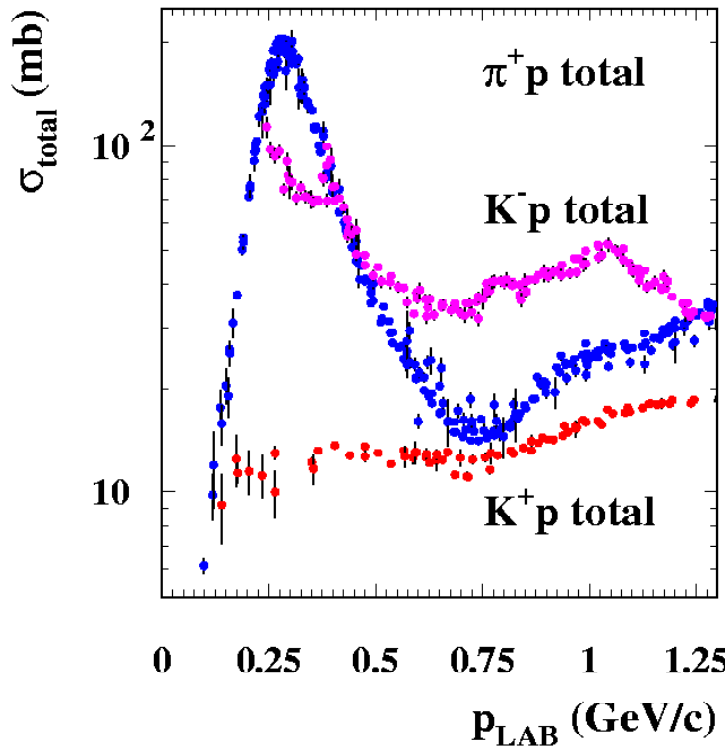


I. Cluster, hyperon and hypercluster production via HICs and hadron induced reactions

1. Strange particle production in hadron-hadron collisions

科学出版社
 2018年 第63卷 第8期 : 735~744
 论文

SCIENCE CHINA PRESS

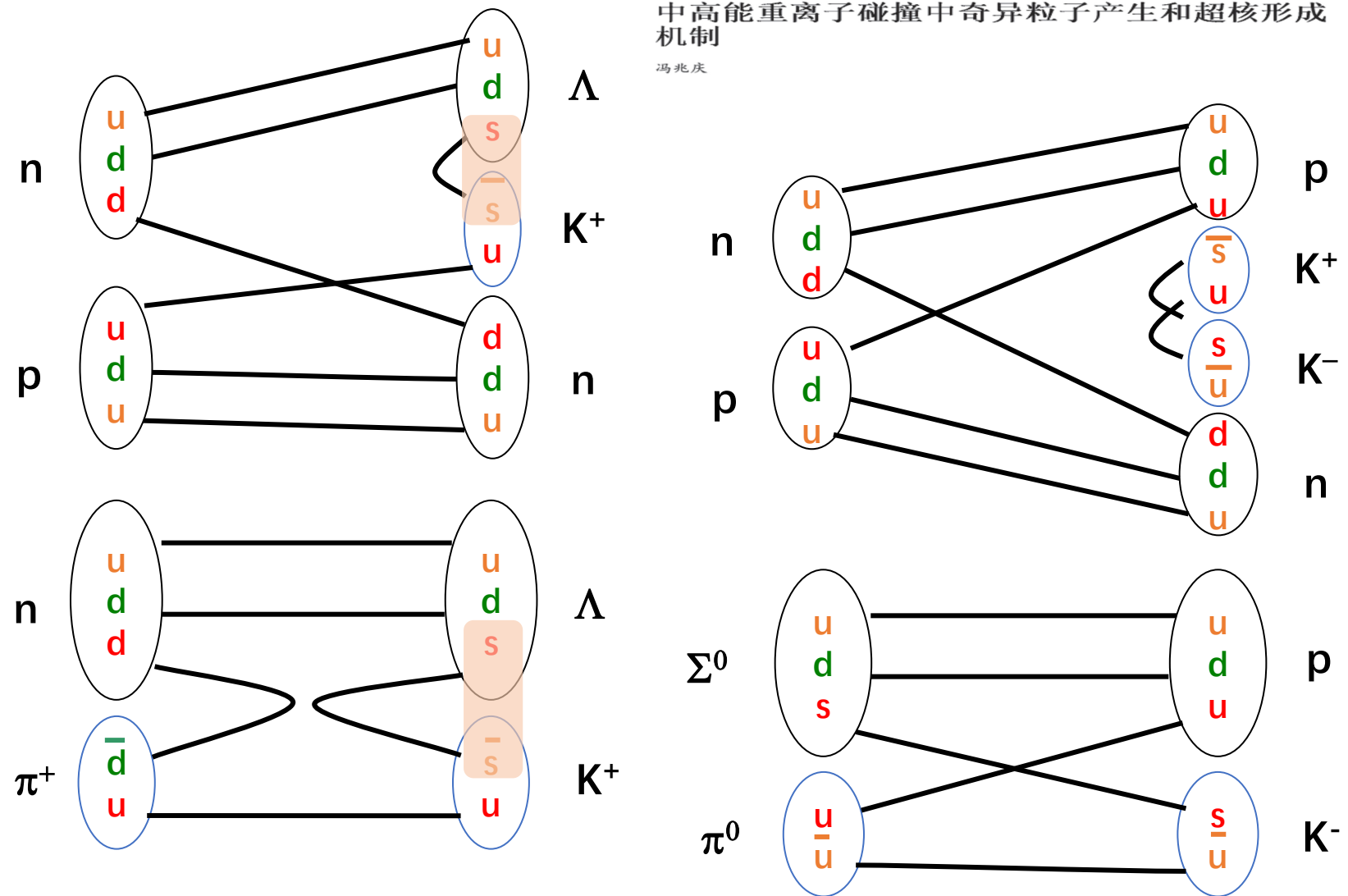


mean free path at ρ_0 :

$$\lambda(\pi) = 0.3 \text{ fm}$$

$$\lambda(K^+) = 5 \text{ fm}$$

$$\lambda(K^-) = 0.8 \text{ fm}$$



2. Cluster production in heavy-ion collisions

Experiments:

SSC and CSR(HIRFL), INDRA (GANIL), CHIMERA (LNS), NSCL (MSU), FOPI and HADES (GSI) ...

Cluster production measurement at FOPI

Multiplicities and charge balance for Au + Au at $E/A = 0.15$ GeV and $b_0 < 0.15$.

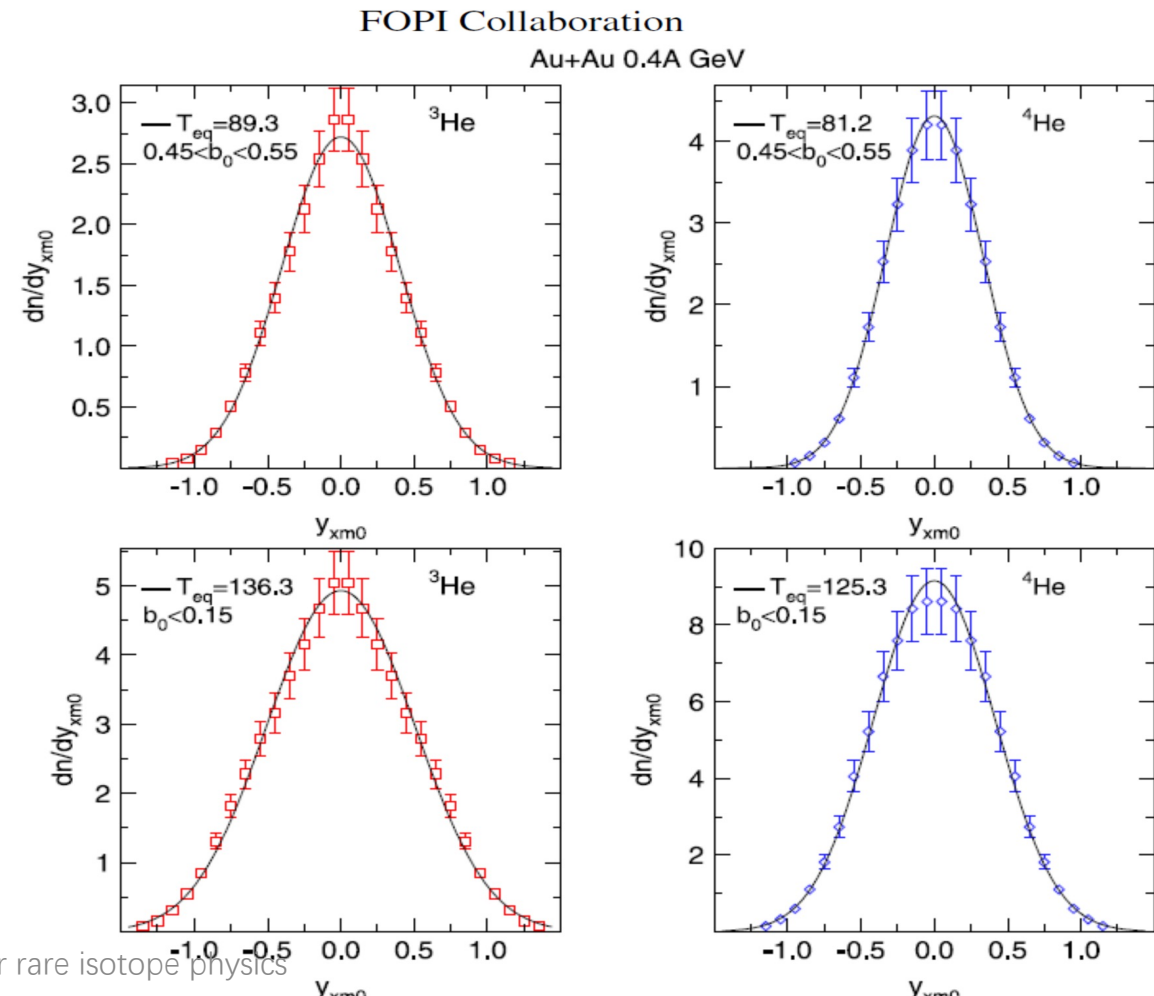
Z = 1	59.9 ± 3.0	p	24.1 ± 1.2	Z = 2	25.0 ± 1.8	${}^3\text{He}$	8.4 ± 0.9
d	20.4 ± 1.4				${}^4\text{He}$	16.6 ± 1.7	
t	15.1 ± 1.5						
Li	5.0 ± 0.5	Be	1.69 ± 0.17				
B	1.44 ± 0.15	C	0.90 ± 0.09				
N	0.50 ± 0.05	O	0.26 ± 0.03				

Multiplicities and charge balance for Ni + Ni at $E/A = 0.25$ GeV and $b_0 < 0.15$.

Z = 1	34.9 ± 1.8	p	19.2 ± 1.0	Z = 2	9.0 ± 0.7	${}^3\text{He}$	3.24 ± 0.33
d	10.5 ± 0.8				${}^4\text{He}$	5.79 ± 0.58	
t	5.1 ± 0.5						
Li	0.91 ± 0.09	Be	0.26 ± 0.03				
B	0.10 ± 0.01						

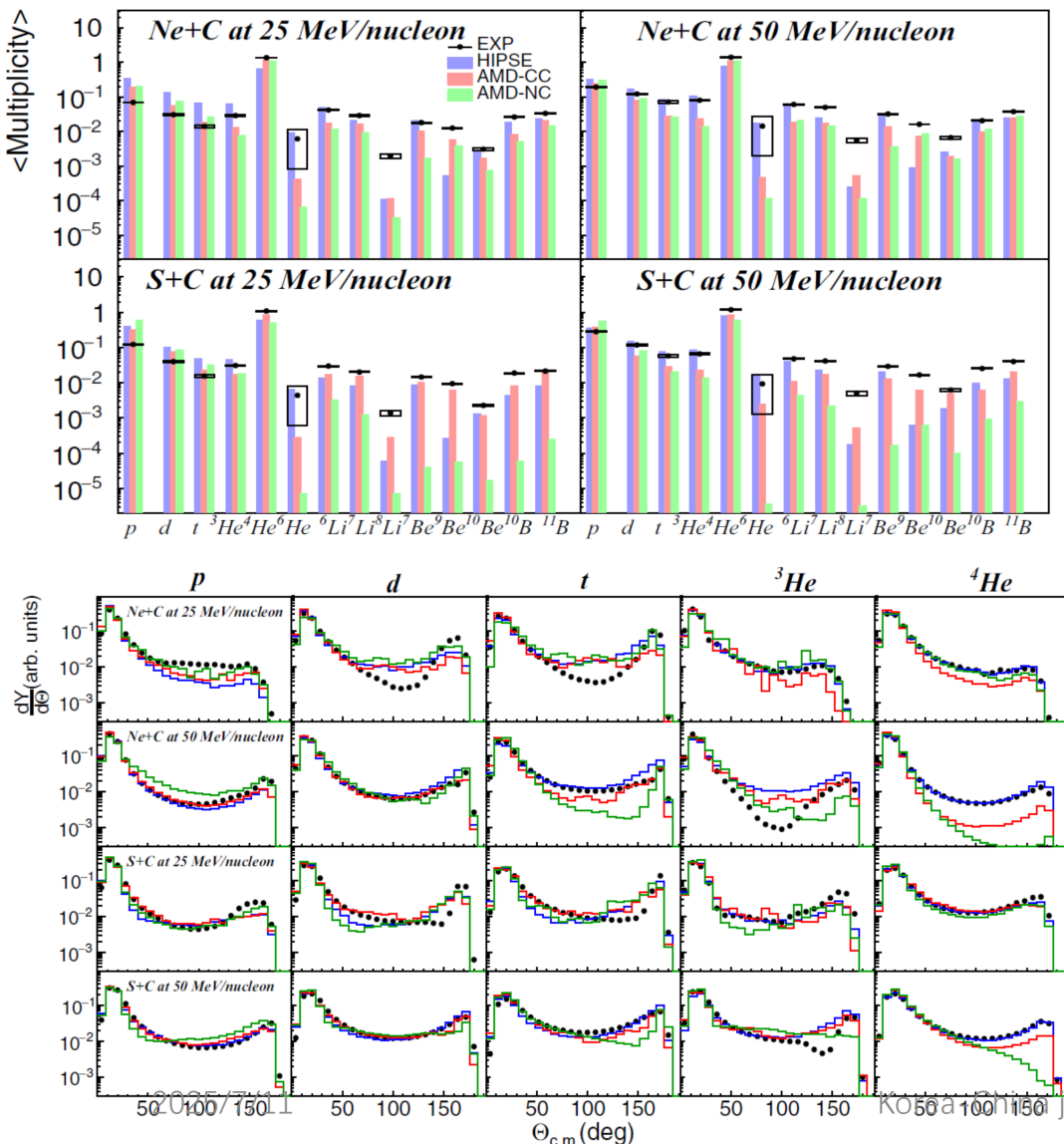


Systematics of central heavy ion collisions in the 1A GeV regime



Cluster production measurement by INDRA-FAZIA at INFN-LNS

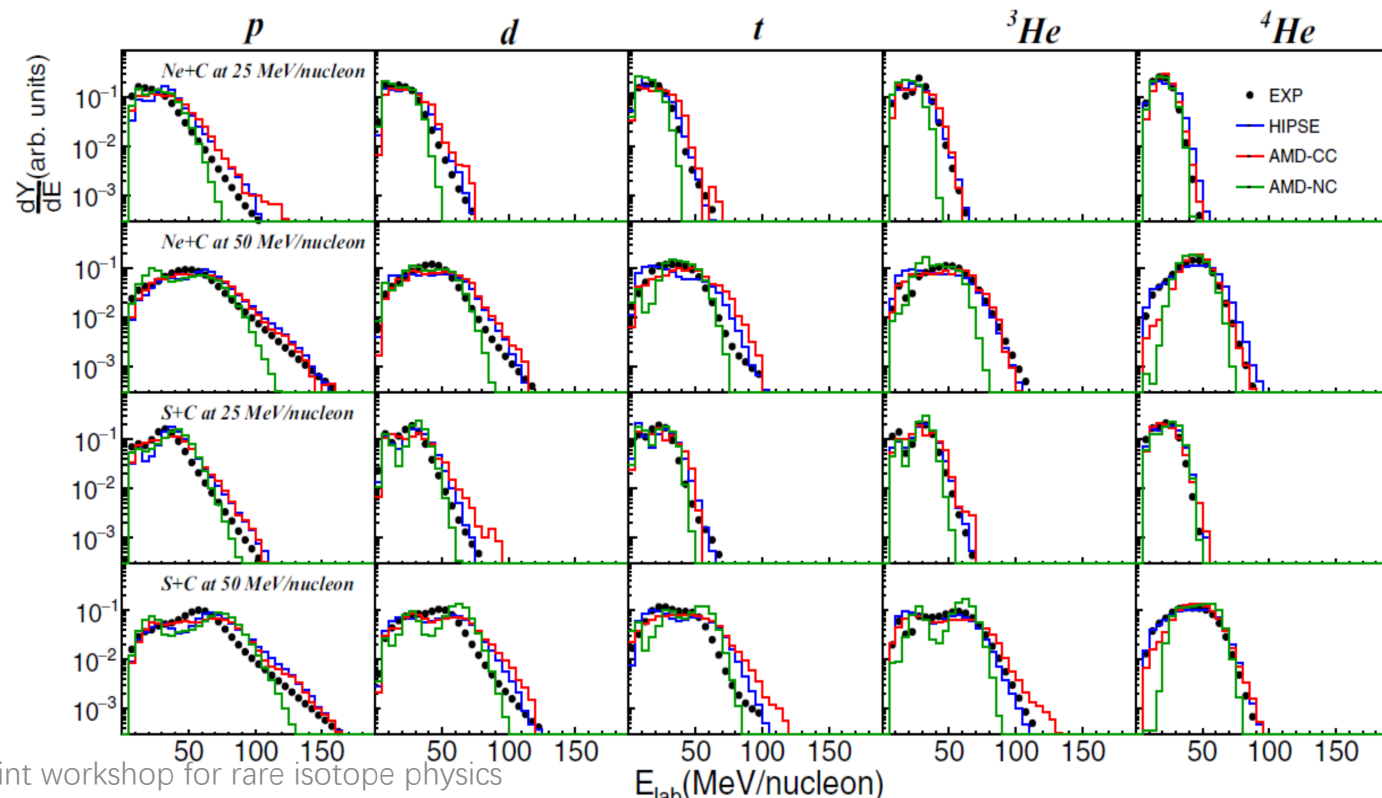
Featured in Physics



Examination of cluster production in excited light systems at Fermi energies from new experimental data and comparison with transport model calculations

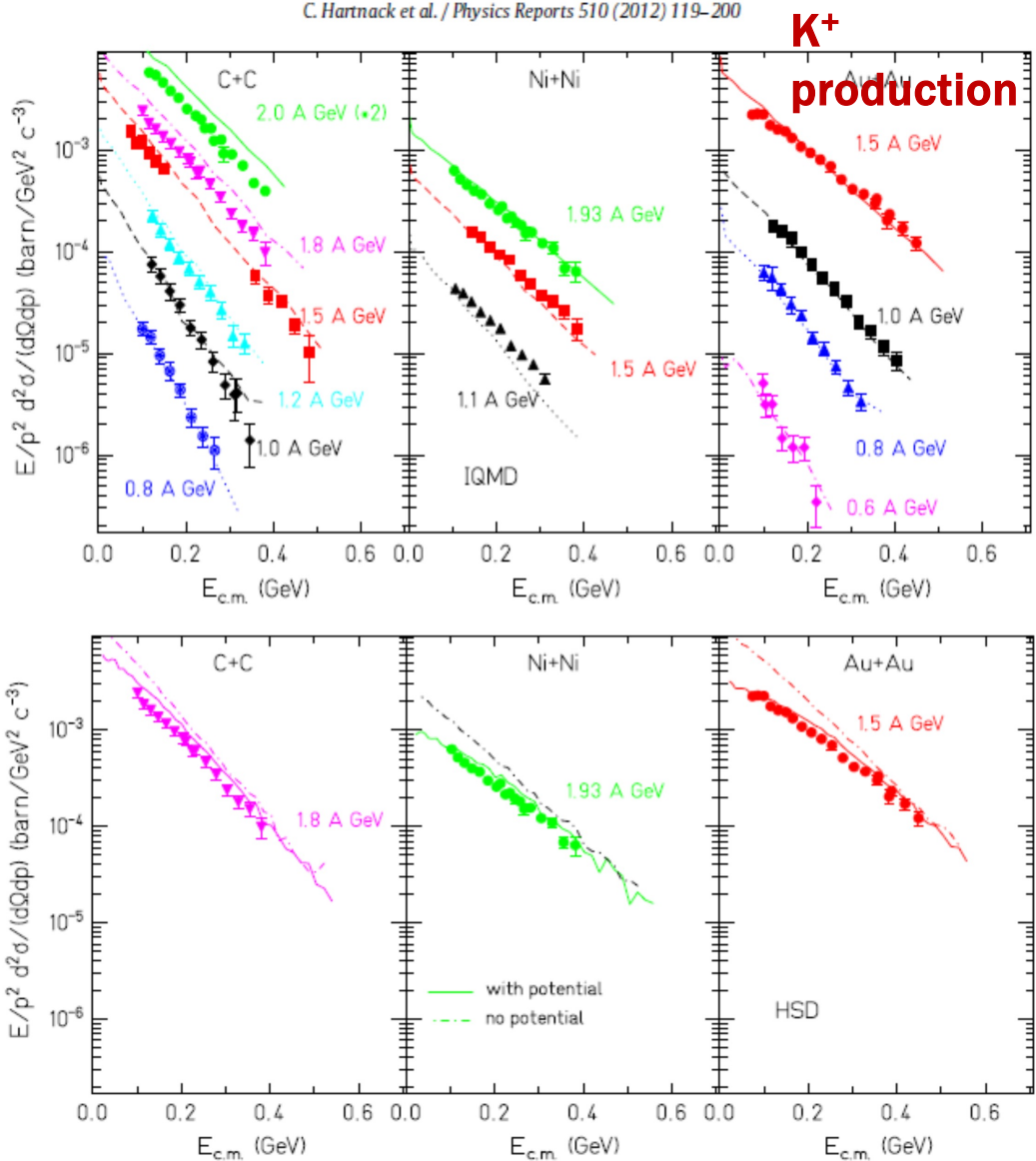
C. Frosin^{1,2,*}, S. Piantelli,² G. Casini,² A. Ono,³ A. Camaiani,⁴ L. Baldesi,² S. Barlini,^{1,2} B. Borderie,⁵ R. Bougault,⁶ C. Ciampi,^{1,2} M. Cicerchia,⁷ A. Chbihi,⁸ D. Dell'Aquila,^{9,10} J. A. Dueñas,¹¹ D. Fabris,¹² Q. Fable,¹³ J. D. Frankland,⁸ T. Génard,⁸ F. Gramegna,⁷ D. Gruyer,⁶ M. Henri,⁸ B. Hong,^{14,15} M. J. Kweon,¹⁶ S. Kim,¹⁷ A. Kordyasz,¹⁸ T. Kozik,¹⁹ I. Lombardo,^{20,21} O. Lopez,⁶ T. Marchi,⁷ K. Mazurek,²² S. H. Nam,^{14,15} J. Lemarié,⁸ N. LeNeindre,⁶ P. Ottanelli,² M. Parlog,^{6,23} J. Park,^{14,15} G. Pasquali,^{1,2} G. Poggi,^{1,2} A. Rebillard-Soulié,⁶ B. H. Sun,²⁴ A. A. Stefanini,^{1,2} S. Terashima,²⁴ S. Upadhyaya,¹⁹ S. Valdré,² G. Verde,^{20,13} E. Vient,⁶ and M. Vigilante^{25,26}

(INDRA-FAZIA Collaboration)

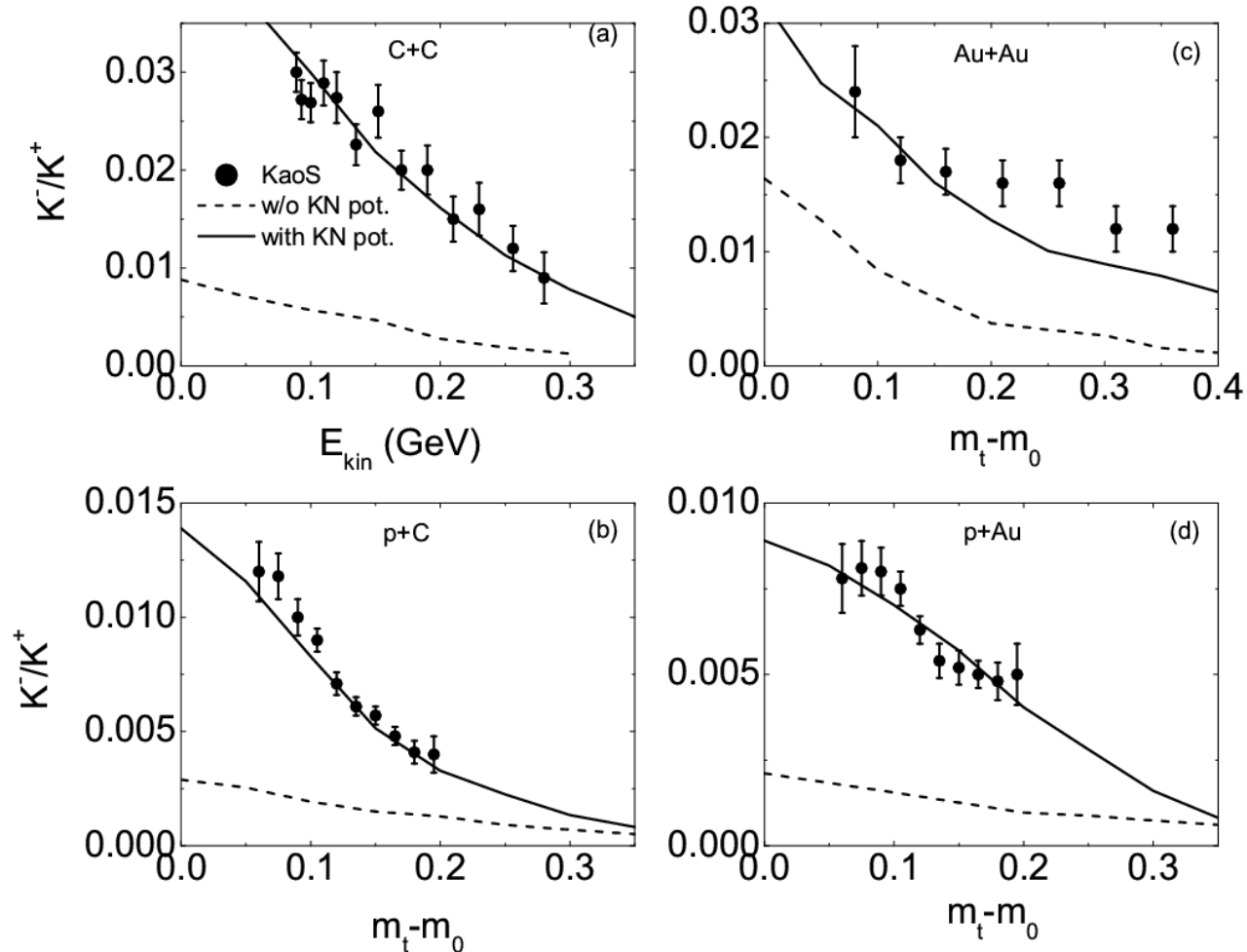


3. Strange particle production in HICs

C. Hartnack et al. / Physics Reports 510 (2012) 119–200



The ratio of K^-/K^+ in HICs of $^{12}\text{C} + ^{12}\text{C}$ ($^{197}\text{Au} + ^{197}\text{Au}$) at 1.8A GeV and proton beams at 2.5 GeV
(Z. Q. Feng et al., Phys. Rev. C 90, 064604 (2014))

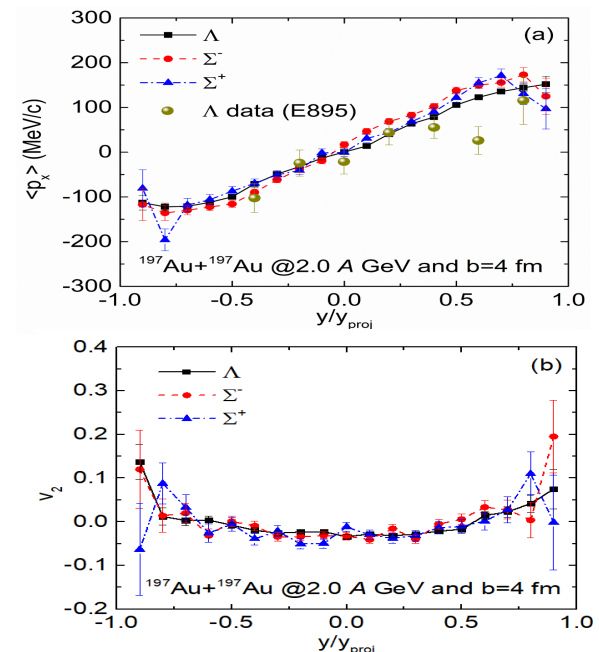
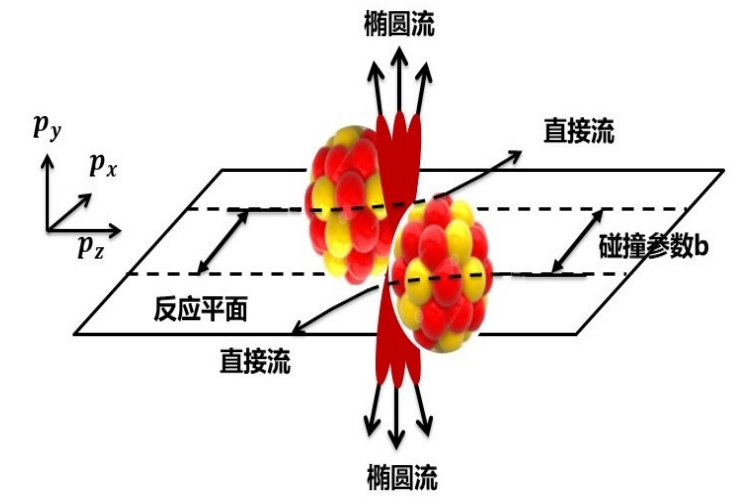
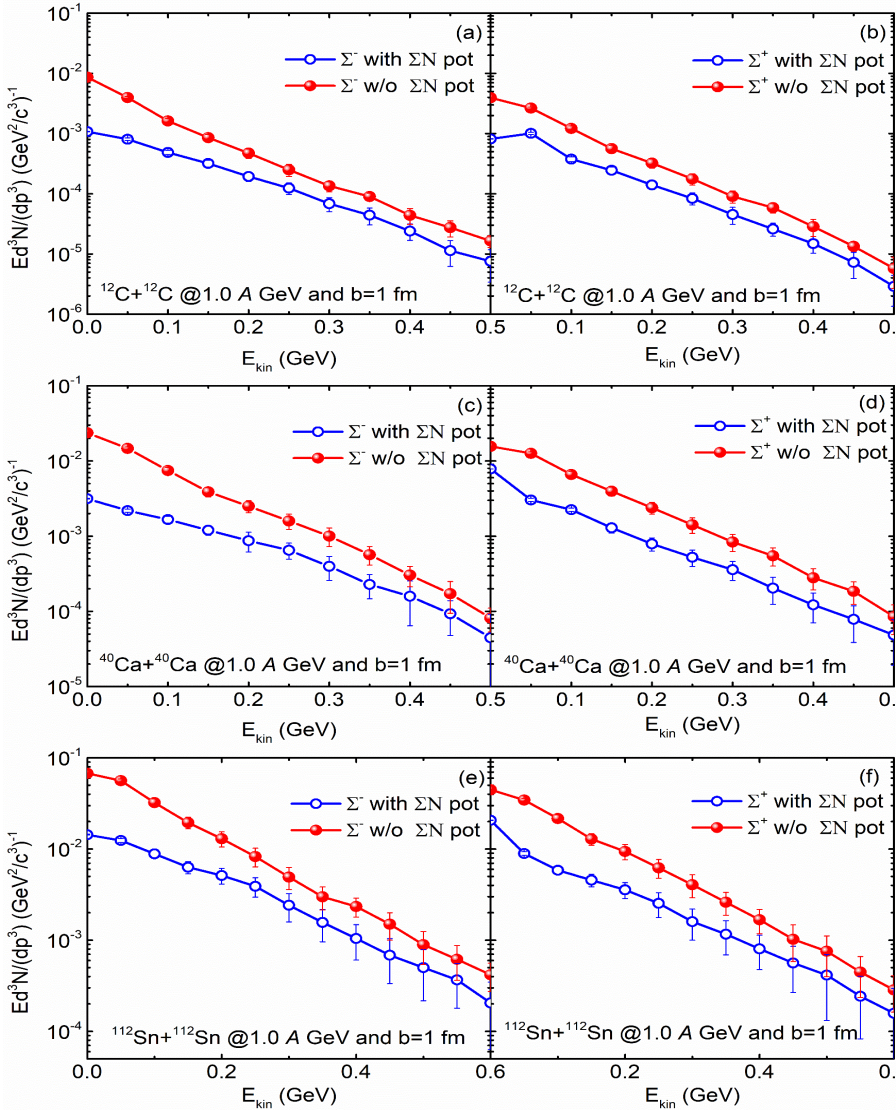
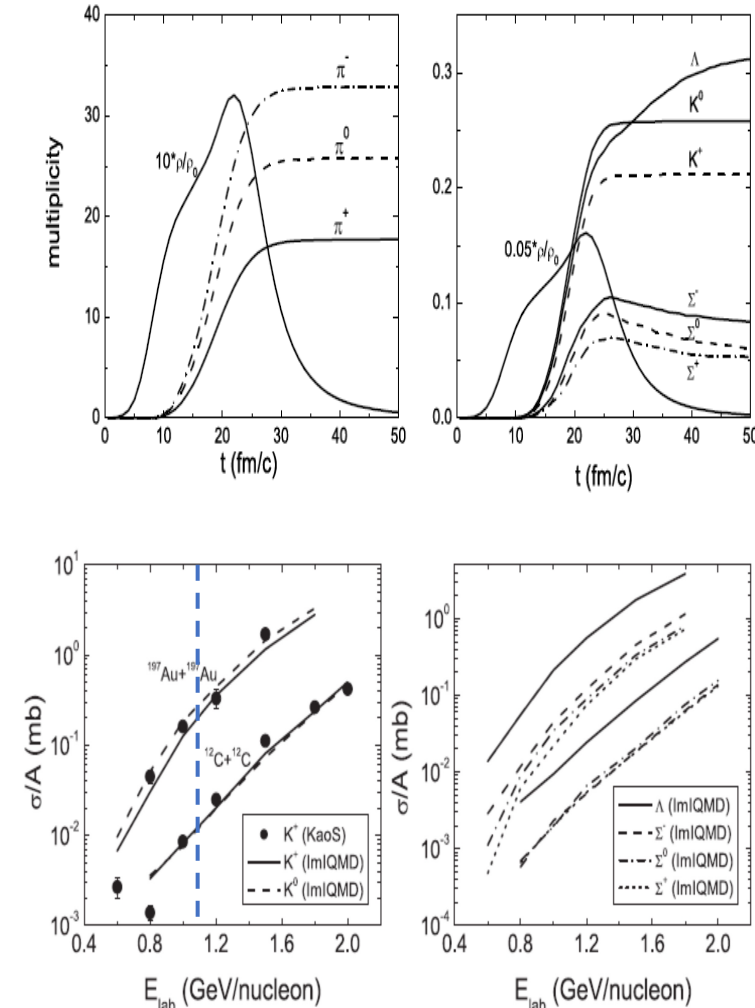


$$V_{K^+}(p_0) = 28 \text{ MeV}, \quad V_{K^-}(p_0) = -100 \text{ MeV}$$

Kaon and hyperon production in HICs (yields, invariant energy spectra, collective flows)

ZQF, Phys. Rev. C 82 (2010) 057901; Phys. Rev. C 87 (2013) 064605; Ding-Chang Zhang et al., Chin. Phys. Lett. 38 (2021) 092501

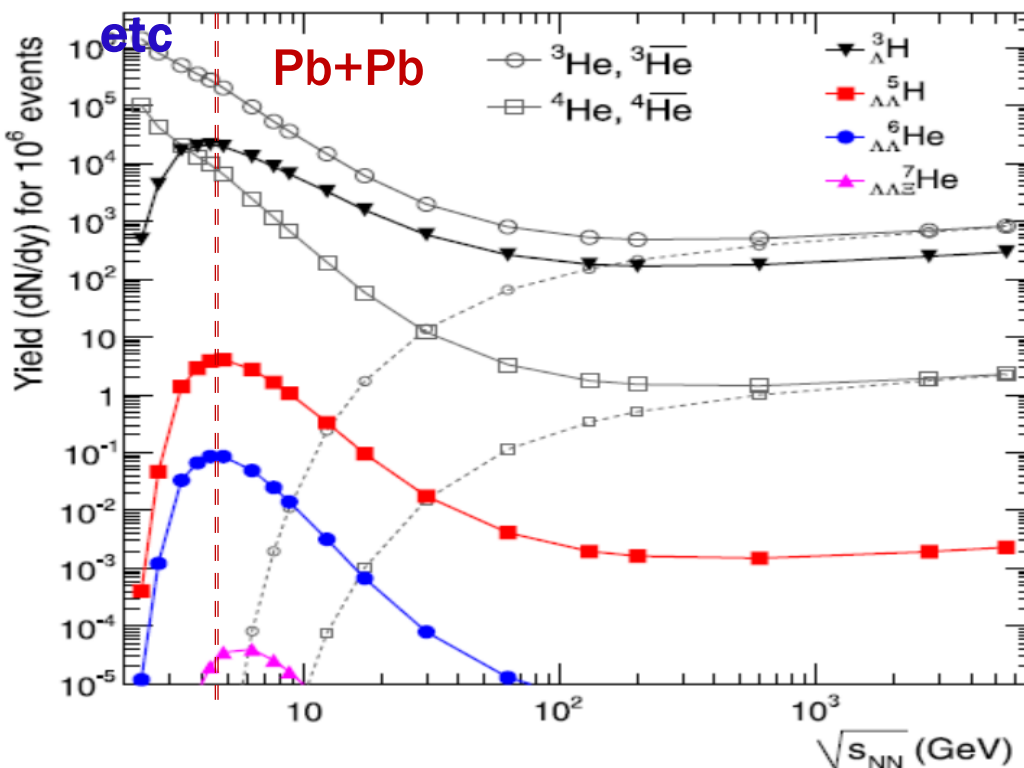
$^{197}\text{Au}+^{197}\text{Au}$ @ 1.54 GeV



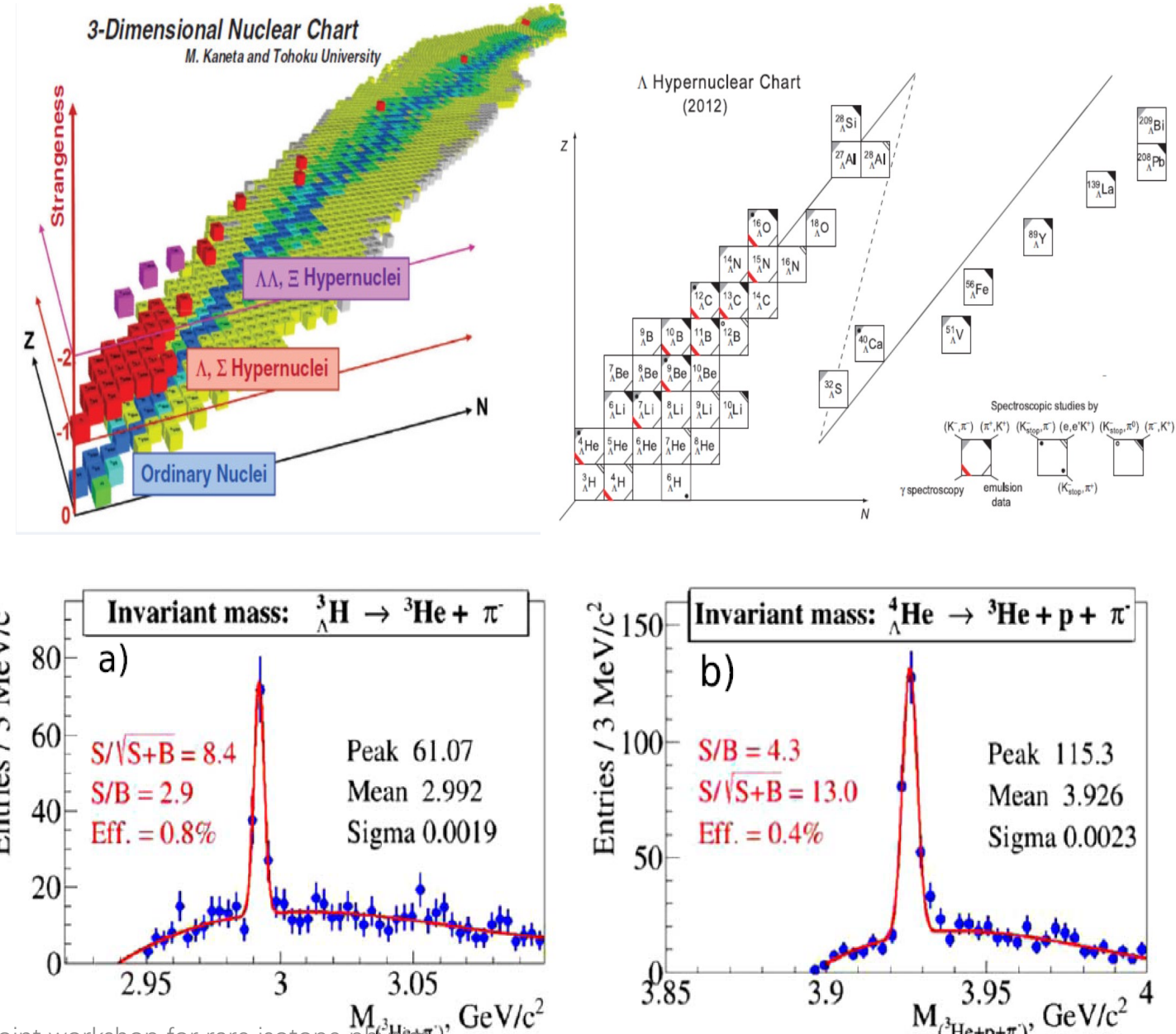
5. Hypernuclear production in HICs

H. Tamura, *Prog. Theor. Exp. Phys.* (2012) 02B012

- ① Neutron-rich/proton-rich HN nuclei and spectroscopies
- ② Multistrangeness HN ($S=-2$) $\Lambda\Lambda X$ 和 $\Xi\Xi X$
- ③ Interaction potentials of $N\Lambda$, $N\Sigma$ $NN\Lambda$,



A. Andronic, P. Braun-Munzinger, J. Stachel, H. Stöcker,
2025/7/11
Physics Letters B 697 (2011) 203–207



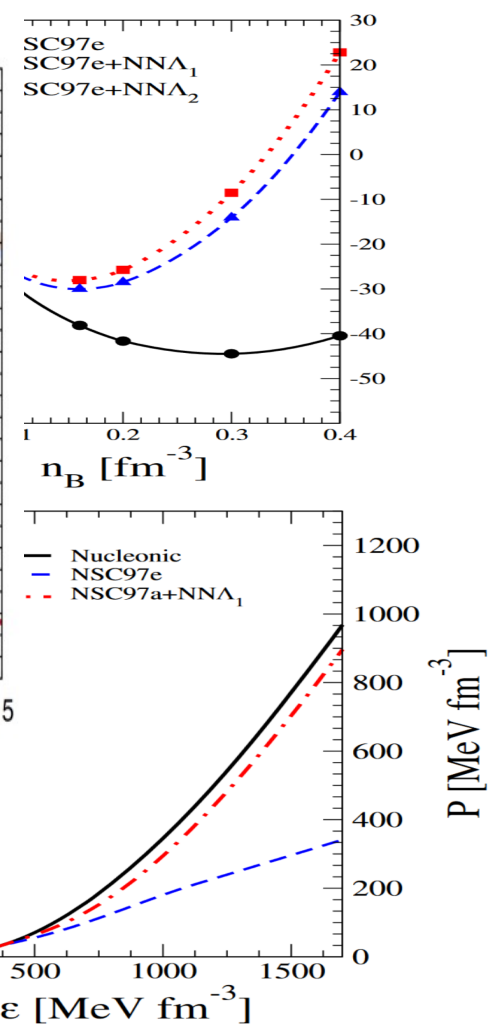
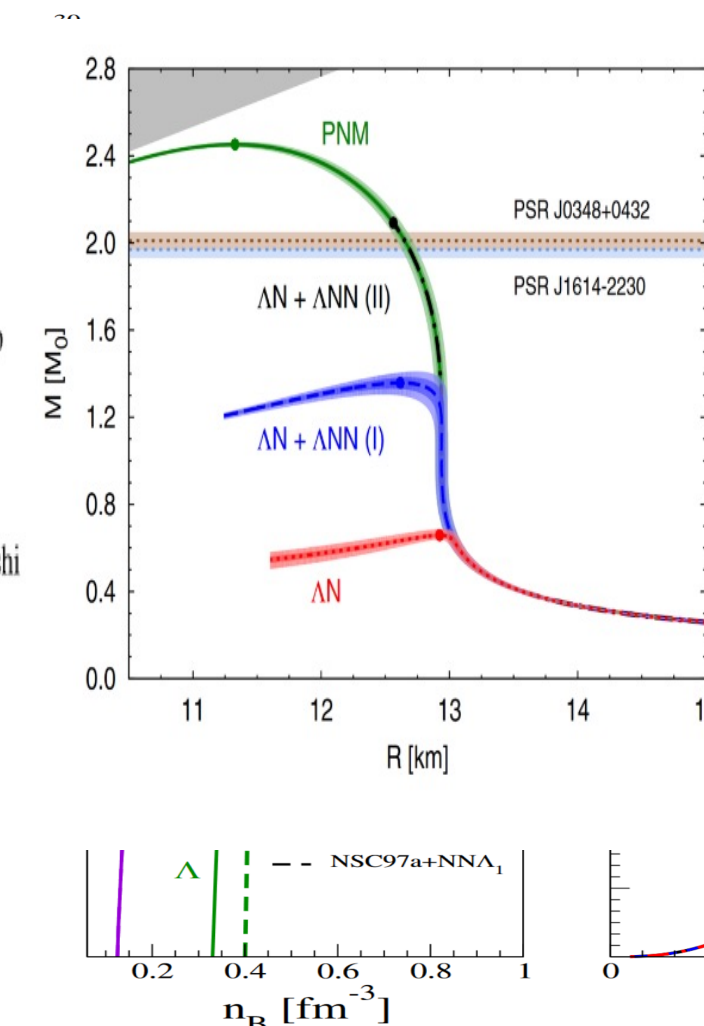
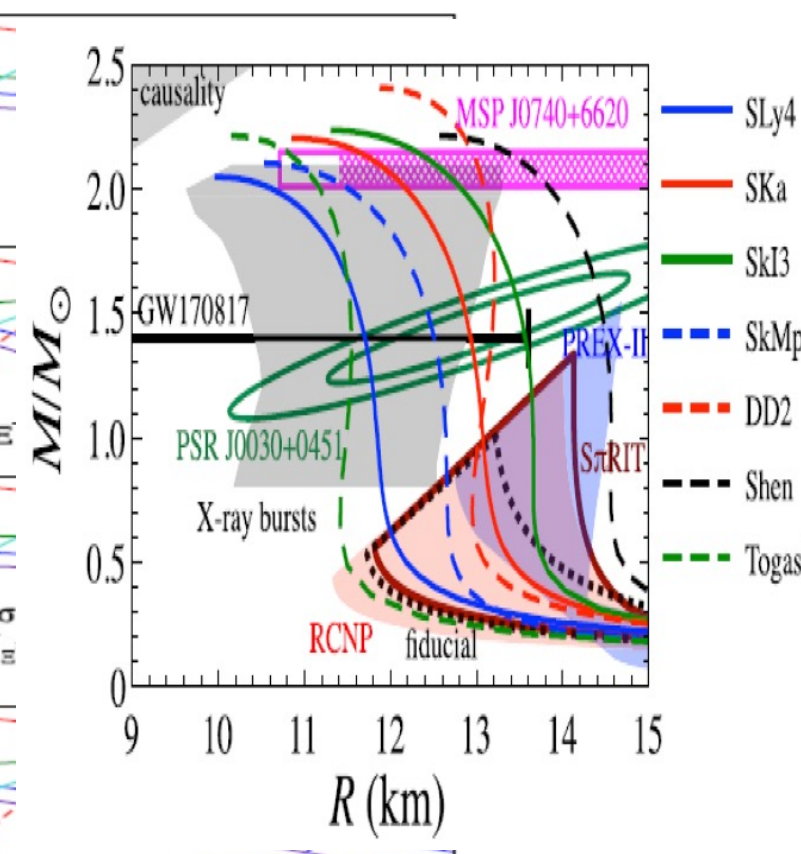
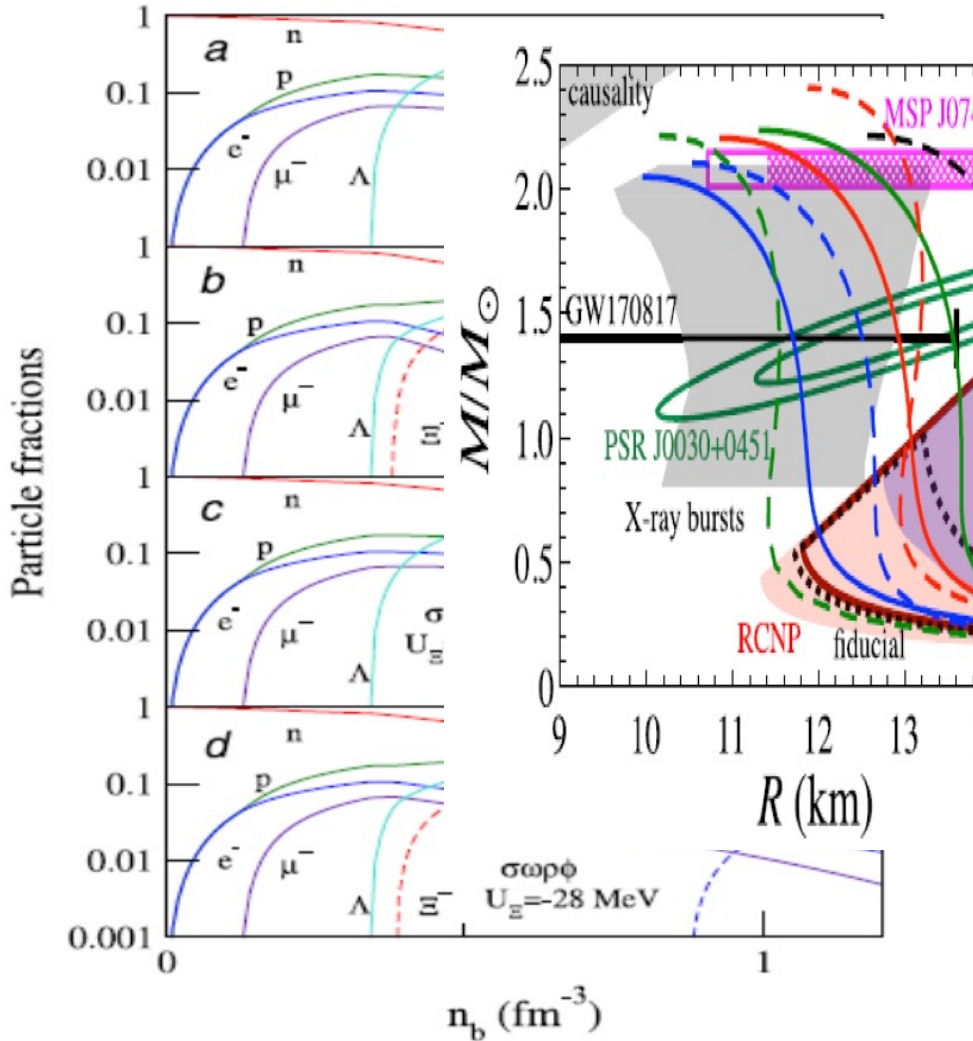
Korea-China joint workshop for rare isotope physics

Hyperons in neutron stars (NS)

S. Weissenborn, D. Chatterjee, J. Schaffner-Bielich, Nucl. Phys. A 881, 62 (2012)

W. Z. Jiang, R. Y. Yang, and D. R. Zhang, Phys. Rev. C 87, 064314 (2013)

Diego Lonardoni, Alessandro Lovato, Stefano Gandolfi, and Francesco Pederiva, Phys. Rev. Lett. 114, 092301 (2015)



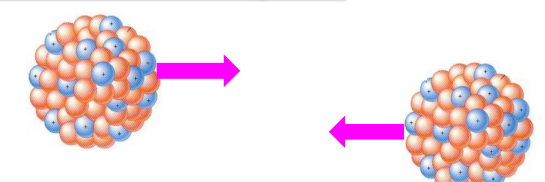
II. LQMD transport model



Lanzhou quantum molecular dynamics transport model (LQMD)

Heavy-ion collisions (5 MeV – 5 GeV/nucleon) and hadron induced reaction (p , \bar{p} , π , K , e , etc)

- **LQMD transport model** (Skyrme interaction, Walecka model with σ , ω , ρ , δ)
- **Neutron star equation of state via HICs** (nuclear symmetry energy at sub- and supra-saturation densities in HICs, isospin splitting of nucleon effective mass from HICs, particle production, 2-body and 3-body potential, multi-body correlation)
- **In-medium effects of hadrons** (optical potentials, energy conservation and in-medium effects, i.e., $\Delta(1232)$, $N^*(1440)$, $N^*(1535)$), hyperons (Λ, Σ, Ξ) and mesons ($\pi, K, \eta, \rho, \omega, \phi, \dots$)
- **Kinetic production of (hyper)clusters and nuclear fragmentation reactions** (production cross section, phase-space distribution, collective flows, cluster transportation, Mott effect, e.g., deuteron, triton, ${}^3\text{He}$, α , $_{\Lambda(\Sigma)}\text{X}$, $_{\Lambda\Lambda}\text{X}$, $_{\Xi}\text{X}$, $_{\bar{\Lambda}}\text{X}$)
- **Nuclear collisions of light systems** (e.g., $d+\alpha$, ${}^9\text{Be}+D_2\text{O}$, $d+{}^7\text{Li}$ etc, antisymmetrization with Volkov 2-body force)
- **Spallation reactions induced by p , d , t , α , \bar{p} , \bar{d} etc (cascade multi-step collision for thick targets)**



1. Lanzhou quantum molecular dynamics transport model (LQMD-Skyrme)

$$H_B = \sum_i \sqrt{\mathbf{p}_i^2 + \mathbf{m}_i^2} + U_{\text{int}} + U_{\text{mom}}$$

$$U_{\text{loc}} = \int V_{\text{loc}}(\rho(\mathbf{r})) d\mathbf{r}$$

PHYSICAL REVIEW C 84, 024610 (2011)

Momentum dependence of the symmetry potential and its influence on nuclear reactions

Zhao-Qing Feng*

Institute of Modern Physics, Chinese Academy of Sciences, Lanzhou 730000, People's Republic of China

(Received 11 July 2011; published 19 August 2011)

$$V_{\text{loc}}(\rho) = \frac{\alpha}{2} \frac{\rho^2}{\rho_0} + \frac{\beta}{1+\gamma} \frac{\rho^{1+\gamma}}{\rho_0^\gamma} + E_{\text{sym}}^{\text{loc}}(\rho) \rho \delta^2 + \frac{g_{\text{sur}}}{2\rho_0} (\nabla \rho)^2 + \frac{g_{\text{sur}}^{\text{iso}}}{2\rho_0} [\nabla(\rho_n - \rho_p)]^2,$$

Phys. Rev. C 84, 024610
(2011); 85, 014604 (2012)

$$U_{\text{mom}} = \frac{1}{2\rho_0} \sum_{i,j,j \neq i} \sum_{\tau,\tau'} C_{\tau,\tau'} \delta_{\tau,\tau_i} \delta_{\tau',\tau_j} \iiint d\mathbf{p} d\mathbf{p}' d\mathbf{r} f_i(\mathbf{r}, \mathbf{p}, t) \\ \times [\ln(\epsilon(\mathbf{p} - \mathbf{p}')^2 + 1)]^2 f_j(\mathbf{r}, \mathbf{p}', t).$$

$C_{\text{sym}} = 38 \text{ MeV}$

$a_{\text{sym}} = 37.7 \text{ MeV}$

$b_{\text{sym}} = -18.7 \text{ MeV}$

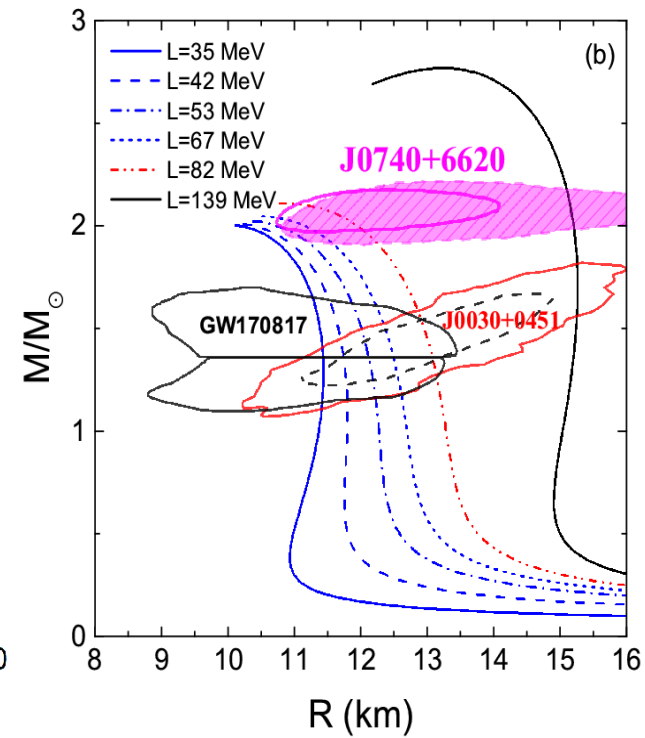
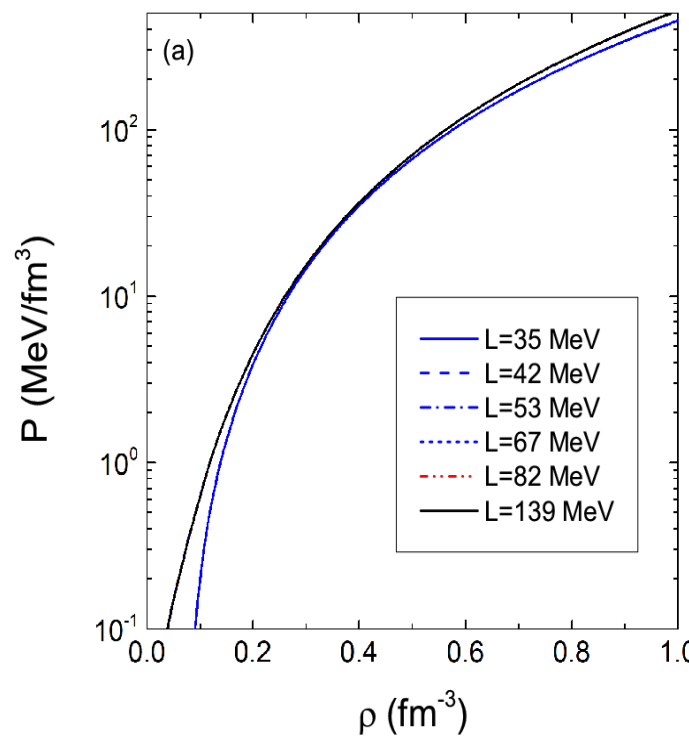
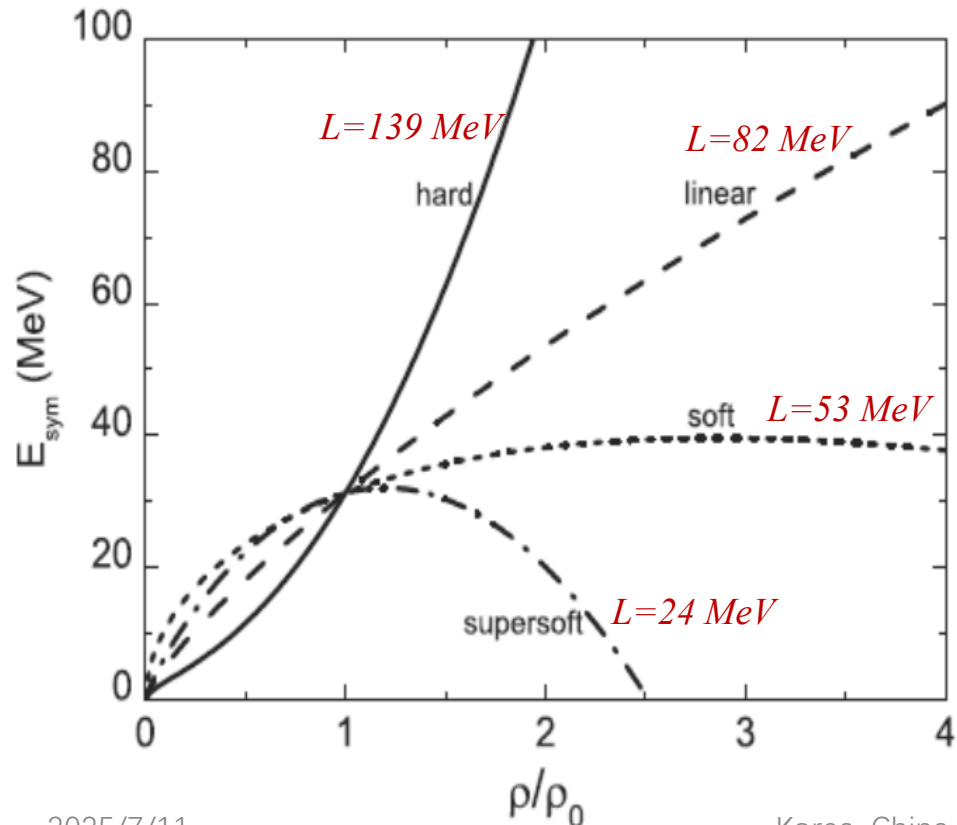
$$E_{\text{sym}}(\rho) = \frac{1}{3} \frac{\hbar^2}{2m} \left(\frac{3}{2} \pi^2 \rho \right)^{2/3} + E_{\text{sym}}^{\text{loc}}(\rho) + E_{\text{sym}}^{\text{mom}}(\rho).$$

$$E_{\text{sym}}^{\text{loc}}(\rho) = \frac{1}{2} C_{\text{sym}} (\rho / \rho_0)^{\gamma_s}$$

$$E_{\text{sym}}^{\text{loc}}(\rho) = a_{\text{sym}} (\rho / \rho_0) + b_{\text{sym}} (\rho / \rho_0)^2.$$

Table 1: The parameters and properties of isospin symmetric EoS used in the LQMD model at the density of 0.16 fm^{-3} .

Parameters	α (MeV)	β (MeV)	γ	C_{mom} (MeV)	ϵ (c^2/MeV^2)	m_∞^*/m	K_∞ (MeV)
PAR1	-215.7	142.4	1.322	1.76	5×10^{-4}	0.75	230
PAR2	-226.5	173.7	1.309	0.	0.	1.	230



2. Covariant energy-density functional (LQMD.RMF)

Si-Na Wei, Zhao-Qing Feng,
 Nuclear Science and Techniques 35, 15 (2024)
 arXiv:2302.09984

$$\begin{aligned}
 L = & \bar{\psi} [i\gamma_\mu \partial^\mu - (M_N - g_\sigma \varphi - g_\delta \vec{\tau} \cdot \vec{\delta}) - g_\omega \gamma_\mu \omega^\mu - g_\rho \gamma_\mu \vec{\tau} \cdot \vec{b}^\mu] \psi \\
 & + \frac{1}{2} (\partial_\mu \varphi \partial^\mu \varphi - m_\sigma^2 \varphi^2) - U(\varphi) + \frac{1}{2} (\partial_\mu \vec{\delta} \partial^\mu \vec{\delta} - m_\delta^2 \vec{\delta}^2) \\
 & + \frac{1}{2} m_\omega^2 \omega_\mu \omega^\mu - \frac{1}{4} F_{\mu\nu} F^{\mu\nu} + \frac{1}{2} m_\rho^2 \vec{b}_\mu \vec{b}^\mu - \frac{1}{4} \vec{G}_{\mu\nu} \vec{G}^{\mu\nu}
 \end{aligned}$$

Energy density functional

$$\varepsilon = \sum_{i=n,p} 2 \int \frac{d^3 k}{(2\pi)^3} \sqrt{k^2 + M_i^{*2}} + \frac{1}{2} m_\sigma^2 \varphi^2 + U(\varphi) + \frac{1}{2} m_\omega^2 \omega_0^2 + \frac{1}{2} m_\rho^2 b_0^2 + \frac{1}{2} m_\delta^2 \delta_0^2$$

$$\begin{aligned}
 F_{\mu\nu} &= \partial_\mu \omega_\nu - \partial_\nu \omega_\mu, \\
 G_{\mu\nu} &= \partial_\mu \vec{b}_\nu - \partial_\nu \vec{b}_\mu, \\
 U(\varphi) &= \frac{g_2}{3} \varphi^3 + \frac{g_3}{4} \varphi^4
 \end{aligned}$$

Temporal evolution in phase space

$$\begin{aligned}
 \dot{\mathbf{x}} = & \frac{\mathbf{p}_i^*}{p_0^*} + \sum_{i \neq j}^N \left\{ \frac{g_v^2}{2m_v^2} z_j^{*\mu} u_{i,\mu} B_i B_j \frac{\partial \rho_{ij}}{\partial \mathbf{p}_i} + \frac{g_v^2}{2m_v^2} z_i^{*\mu} u_{j,\mu} B_i B_j \frac{\partial \rho_{ji}}{\partial \mathbf{p}_i} + \frac{g_v^2}{2m_v^2} z_j^{*\mu} \rho_{ji} B_i B_j \frac{\partial u_{i,\mu}}{\partial \mathbf{p}_i} \right. \\
 & + z_j^{*\mu} \frac{B_i B_j \bar{g}_v^2}{2m_v^2} \left[\frac{\rho_{ij}}{1 - p_{T,ij}^2/\Lambda_v^2} \frac{\partial u_{i,\mu}}{\partial \mathbf{p}_i} + \frac{u_{i,\mu}}{1 - p_{T,ij}^2/\Lambda_v^2} \frac{\partial \rho_{ij}}{\partial \mathbf{p}_i} + u_{i,\mu} \rho_{ij} \frac{\partial [1/(1 - p_{T,ij}^2/\Lambda_v^2)]}{\partial \mathbf{p}_i} \right] \\
 & + z_i^{*\mu} \frac{B_i B_j \bar{g}_v^2}{2m_v^2} \left[\frac{u_{j,\mu}}{1 - p_{T,ji}^2/\Lambda_v^2} \frac{\partial \rho_{ji}}{\partial \mathbf{p}_i} + u_{j,\mu} \rho_{ji} \frac{\partial [1/(1 - p_{T,ji}^2/\Lambda_v^2)]}{\partial \mathbf{p}_i} \right] \\
 & \left. - \frac{m_j^*}{p_j^{*0}} \frac{\partial S_j}{\partial \mathbf{p}_i^{5/7}} - \frac{m_i^*}{p_i^{*0}} \frac{\partial S_i}{\partial \mathbf{p}_i} \right\},
 \end{aligned}$$

$$\begin{aligned}
 \dot{\mathbf{p}} = & - \sum_{i \neq j}^N \left\{ \frac{g_v^2}{2m_v^2} z_j^{*\mu} u_{i,\mu} B_i B_j \frac{\partial \rho_{ij}}{\partial \mathbf{r}_i} + \frac{g_v^2}{2m_v^2} z_i^{*\mu} u_{j,\mu} B_i B_j \frac{\partial \rho_{ji}}{\partial \mathbf{r}_i} \right. \\
 & + z_j^{*\mu} \frac{B_i B_j \bar{g}_v^2}{2m_v^2} \frac{u_{i,\mu}}{1 - p_{T,ij}^2/\Lambda_v^2} \frac{\partial \rho_{ij}}{\partial \mathbf{r}_i} \\
 & + z_i^{*\mu} \frac{B_i B_j \bar{g}_v^2}{2m_v^2} \frac{u_{j,\mu}}{1 - p_{T,ji}^2/\Lambda_v^2} \frac{\partial \rho_{ji}}{\partial \mathbf{r}_i} \\
 & \left. - \frac{m_j^*}{p_j^{*0}} \frac{\partial S_j}{\partial \mathbf{r}_i} - \frac{m_i^*}{p_i^{*0}} \frac{\partial S_i}{\partial \mathbf{r}_i} \right\},
 \end{aligned}$$

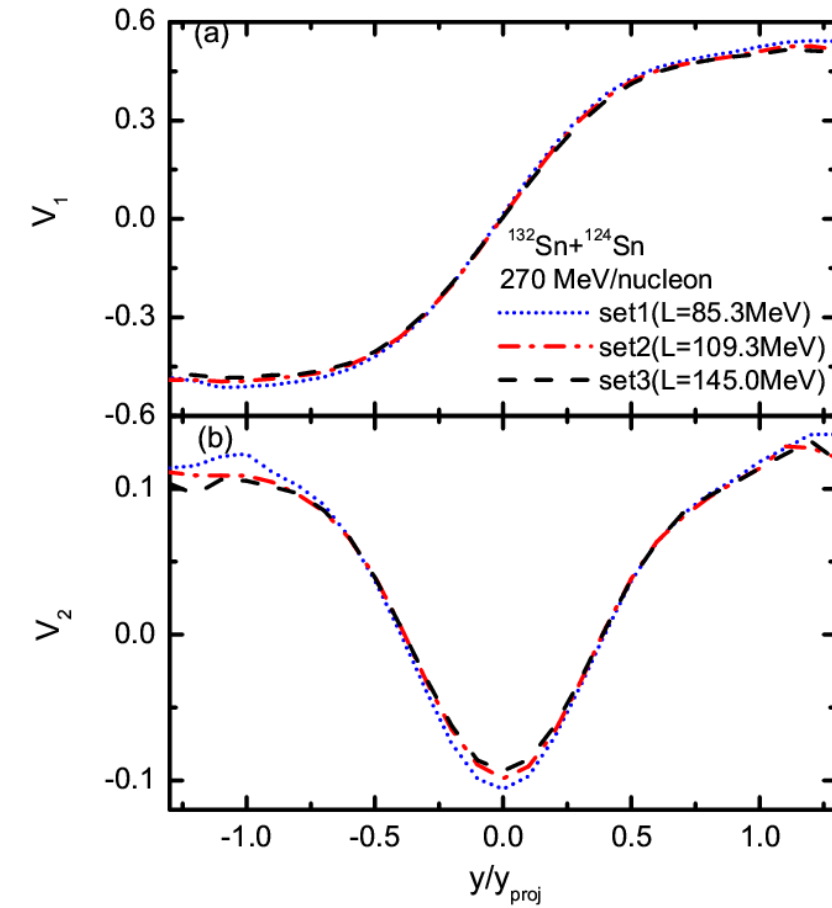
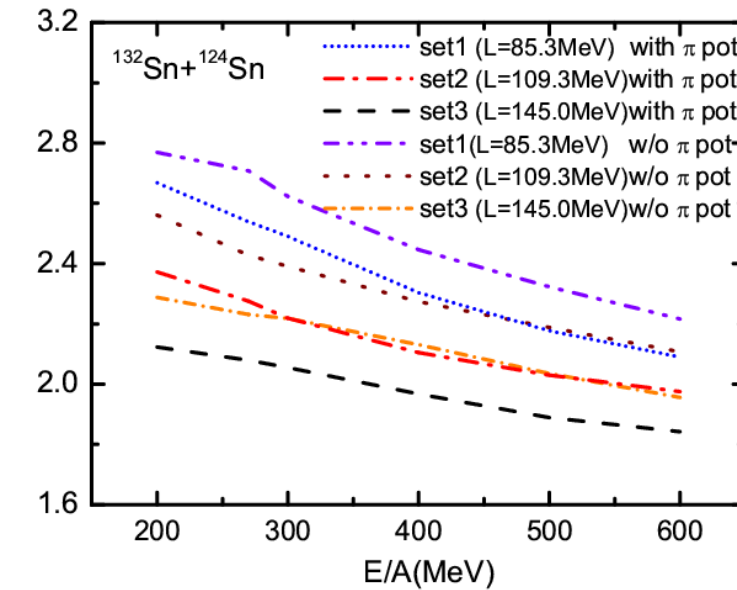
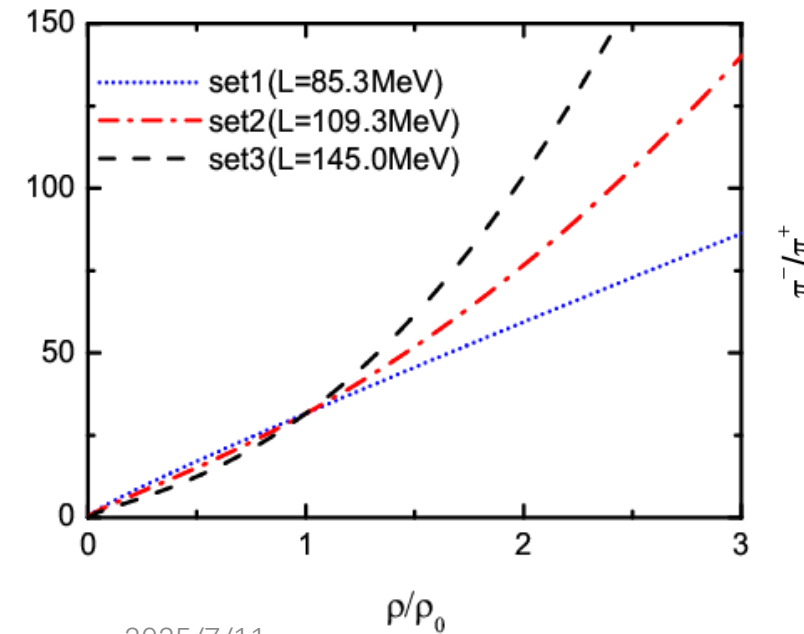
TABLE I: Parameter sets for RMF. The saturation density ρ_0 is set to be 0.16 fm^{-3} . The binding energy of saturation density is $E/A - M_N = -16 \text{ MeV}$. The isoscalar-vector ω and isovector-vector ρ masses are fixed to their physical values, $m_\omega = 783 \text{ MeV}$ and $m_\rho = 763 \text{ MeV}$. The remaining meson mass m_σ is set to be 550 MeV .

model	g_σ	g_ω	$g_2 (\text{fm}^{-1})$	g_3	g_ρ	g_δ	$K (\text{MeV})$	$E_{\text{sym}}(\rho_0) (\text{MeV})$	$L (\rho_0)(\text{MeV})$
set1	8.145	7.570	31.820	28.100	4.049	-	230	31.6	85.3
set2	8.145	7.570	31.820	28.100	8.673	5.347	230	31.6	109.3
set3	8.145	7.570	31.820	28.100	11.768	7.752	230	31.6	145.0

Symmetry
energy

$$E_{\text{sym}} = \frac{1}{6} \frac{k_F^2}{E_F^*} + \frac{1}{2} \left[f_\rho - f_\delta \left(\frac{M^*}{E_F^*} \right) \right] \rho$$

$$f_{\rho,\delta} = g_{\rho,\delta}/m_{\rho,\delta}$$



3. Particle production

π and resonances ($\Delta(1232)$, $N^*(1440)$, $N^*(1535)$, ...) production:

$$\begin{aligned} NN &\leftrightarrow N\Delta, \quad NN \leftrightarrow NN^*, \quad NN \leftrightarrow \Delta\Delta, \quad \Delta \leftrightarrow N\pi, \\ N^* &\leftrightarrow N\pi, \quad NN \leftrightarrow NN\pi(s-state), \quad N^*(1535) \leftrightarrow N\eta \end{aligned}$$

Collisions between resonances, $NN^* \leftrightarrow N\Delta$, $NN^* \leftrightarrow NN^*$

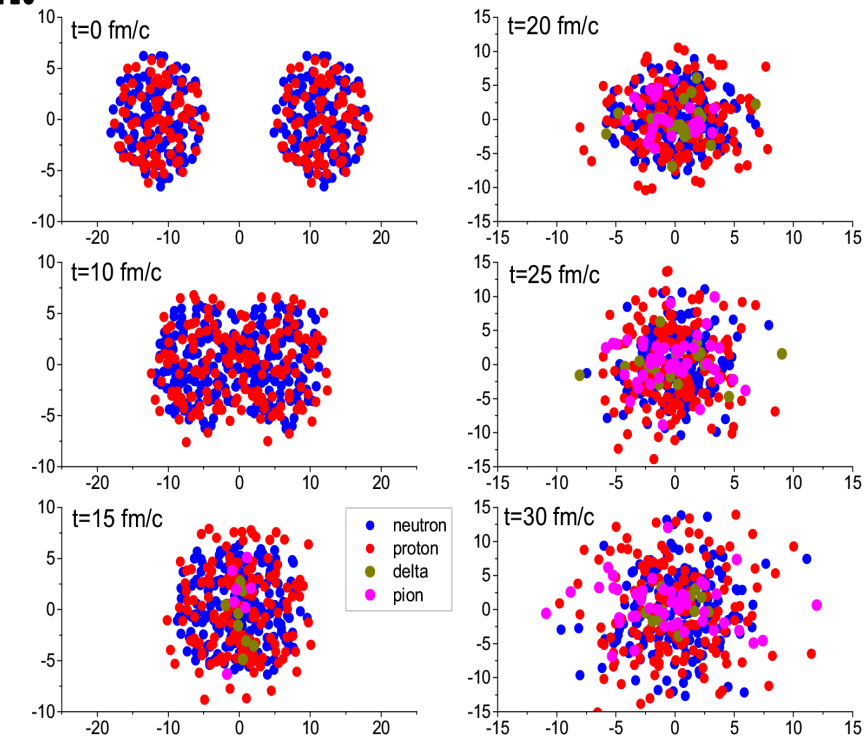
Strangeness channels:

$$\begin{aligned} BB &\rightarrow BYK, BB \rightarrow BB\bar{K}, B\pi(\eta) \rightarrow YK, YK \rightarrow B\pi, \\ B\pi &\rightarrow NK\bar{K}, Y\pi \rightarrow B\bar{K}, \quad B\bar{K} \rightarrow Y\pi, \quad YN \rightarrow \bar{K}NN, \\ BB &\rightarrow B\Xi KK, \bar{K}B \leftrightarrow K\Xi, YY \leftrightarrow N\Xi, \bar{K}Y \leftrightarrow \pi\Xi. \end{aligned}$$

Reaction channels with antiproton:

$$\begin{aligned} \bar{p}N &\rightarrow \bar{N}N, \quad \bar{N}N \rightarrow \bar{N}N, \quad \bar{N}N \rightarrow \bar{B}B, \quad \bar{N}N \rightarrow \bar{Y}Y \\ \bar{N}N &\rightarrow \text{annihilation}(\pi, \eta, \rho, \omega, K, \bar{K}, K^*, \bar{K}^*, \phi) \end{aligned}$$

The PYTHIA and FRITIOF code are used for baryon(meson)-baryon and antibaryon-baryon collisions at high invariant energies



Statistical model with SU(3) symmetry for annihilation
(E.S. Golubeva et al., Nucl. Phys. A 537, 393 (1992))

III. Hyperon-nucleon interaction in dense nuclear matter via HICs

Phys. Lett. B 851 (2024) 138580

$$H_Y = \sum_{i=1}^{N_Y} V_i^{Coul} + V_{opt}^Y(\mathbf{p}_i, \rho_i) + \sqrt{\mathbf{p}_i^2 + m_Y^2}$$

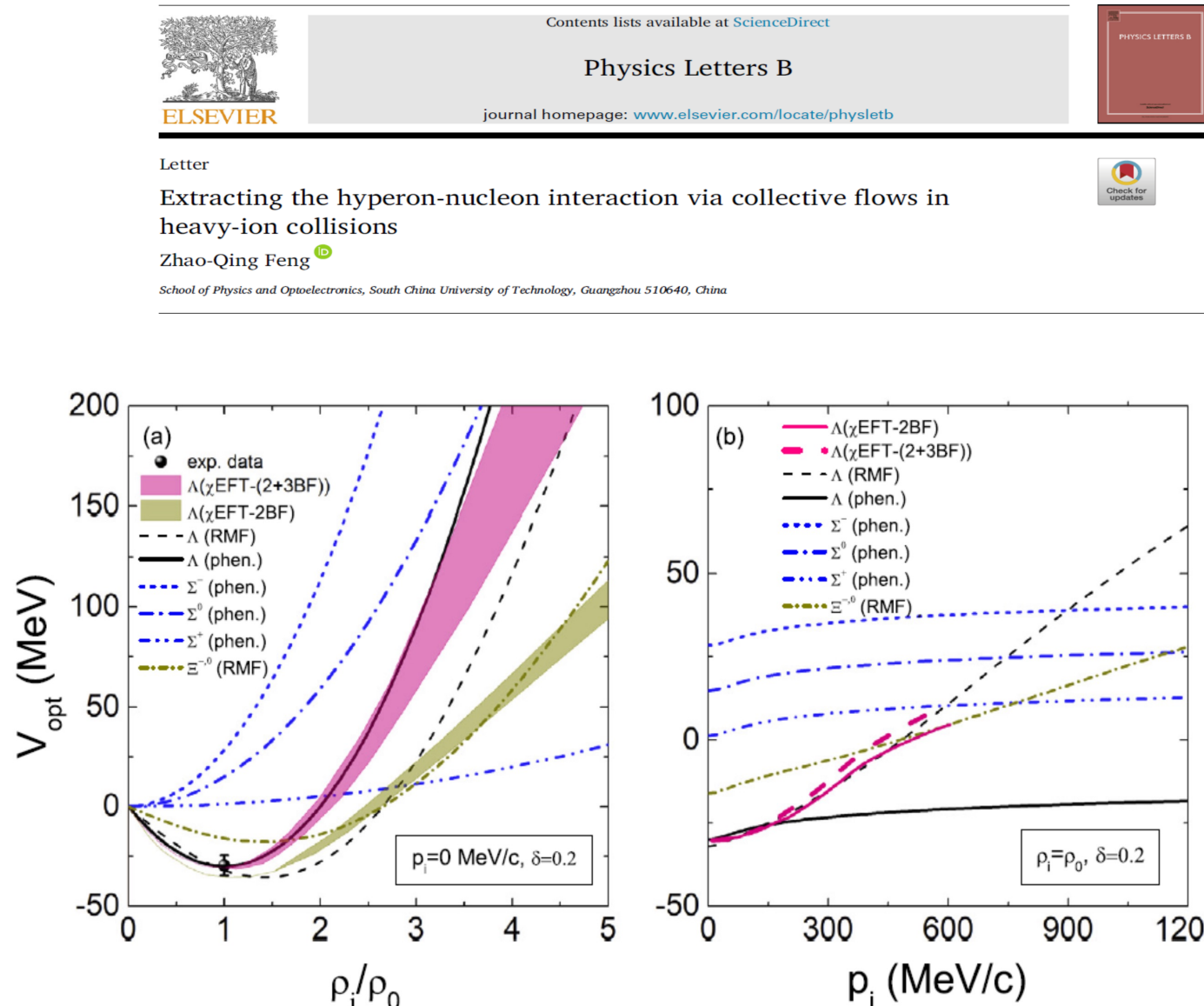
$$V_{opt}^Y(\mathbf{p}_i, \rho_i) = \omega_Y(\mathbf{p}_i, \rho_i) - \sqrt{\mathbf{p}_i^2 + m_Y^2}$$

$$\omega_Y(\mathbf{p}_i, \rho_i) = \sqrt{(m_Y + \Sigma_S^Y)^2 + \mathbf{p}_i^2} + \Sigma_V^Y,$$

Phenomenological potential by fitting
the results of chiral effective field theory

$$V_{opt}^\Lambda(\mathbf{p}_i, \rho_i) = V_a(\rho_i/\rho_0) + V_b(\rho_i/\rho_0)^2 + C_{mom}(\rho_i/\rho_0) \ln(\epsilon \mathbf{p}_i^2 + 1)$$

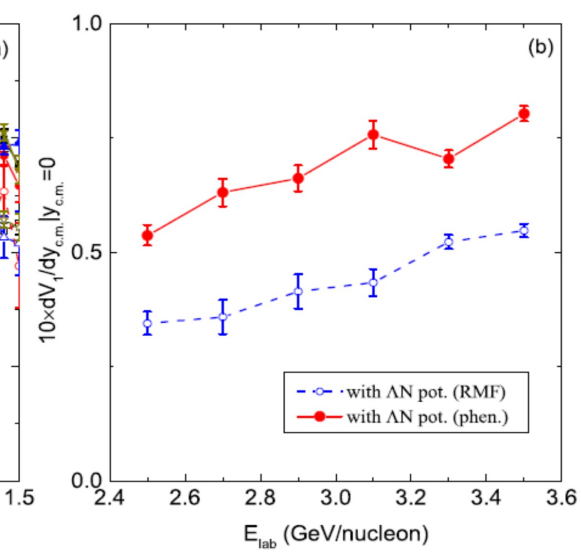
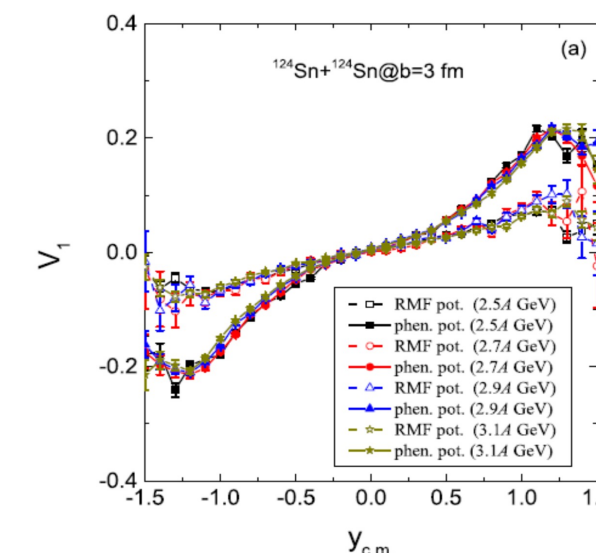
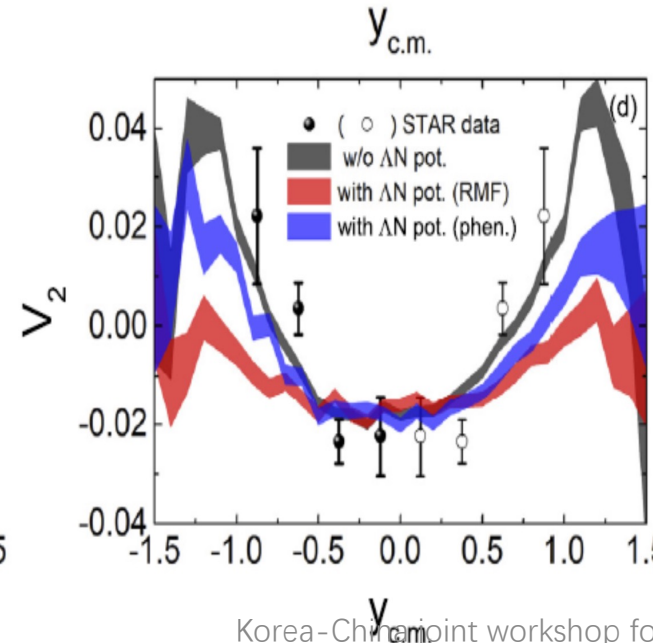
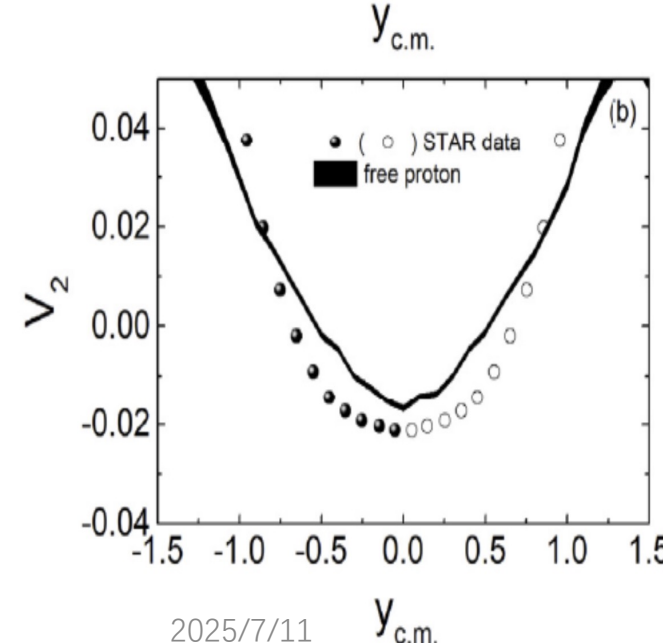
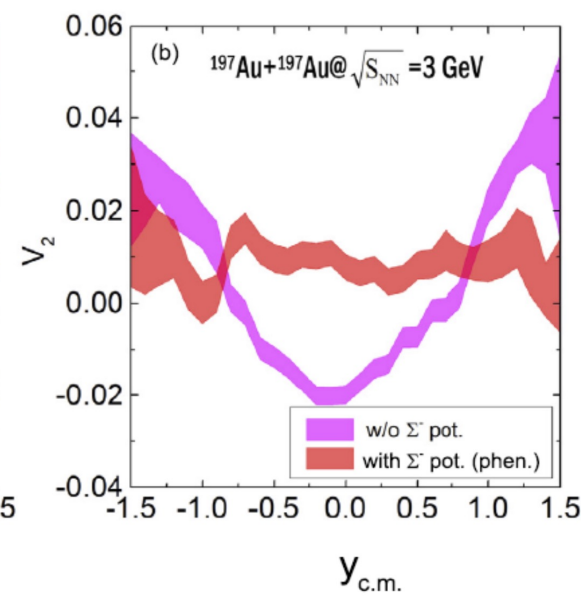
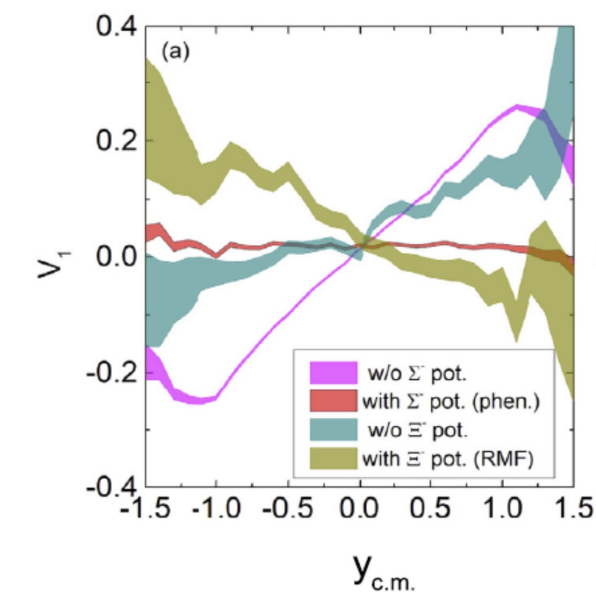
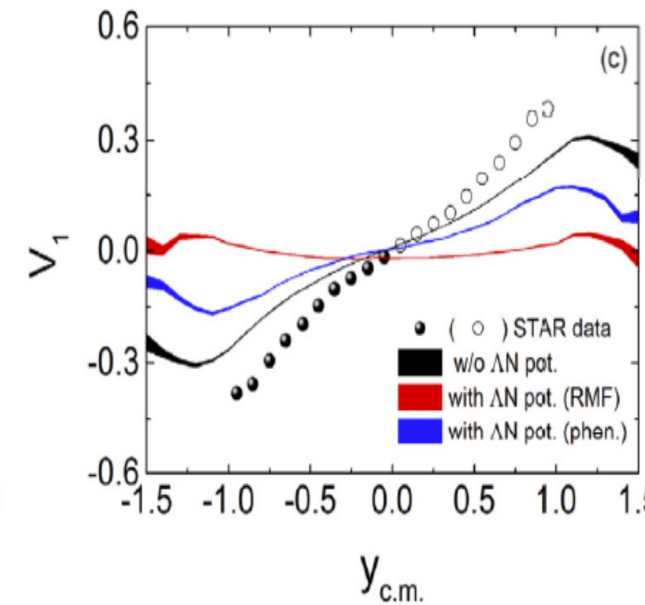
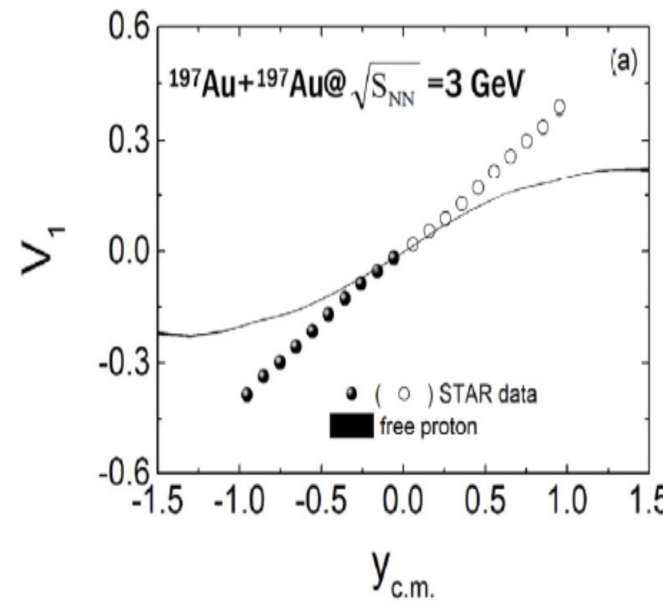
$$V_{opt}^\Sigma(\mathbf{p}_i, \rho_i) = V_0(\rho_i/\rho_0)^{\gamma_s} + V_1(\rho_n - \rho_p)t_\Sigma \rho_i^{\gamma_s^-} + C_{mom}(\rho_i/\rho_0) \ln(\epsilon \mathbf{p}_i^2 + 1).$$



Hyperon-nucleon interaction in dense matter I:

Phys. Lett. B 851 (2024) 138580

Extracting the hyperon-nucleon interaction via collective flows in heavy-ion collisions



Hyperon-nucleon interaction in dense matter I:

The general flavor SU(3) symmetry for hyperon-nucleon potential

$$\mathcal{L}_{int} = \sum_B \bar{\psi}_B [g_{B\sigma}\sigma - \gamma_\mu(g_{B\omega}\omega^\mu + g_{B\phi}\phi^\mu + g_{B\rho}\vec{\tau} \cdot \vec{b}^\mu)]$$

$$]\psi_B - \frac{1}{3}g_2\sigma^3 - \frac{1}{4}g_3\sigma^4,$$

$$\frac{g_{\Lambda\omega}}{g_{N\omega}} = \frac{g_{\Sigma\omega}}{g_{N\omega}} = \frac{\sqrt{2}}{\sqrt{2} + \sqrt{3}z},$$

$$\frac{g_{\Lambda\phi}}{g_{N\omega}} = \frac{g_{\Sigma\phi}}{g_{N\omega}} = \frac{-1}{\sqrt{2} + \sqrt{3}z},$$

$$\frac{g_{\Xi\omega}}{g_{N\omega}} = \frac{\sqrt{2} - \sqrt{3}z}{\sqrt{2} + \sqrt{3}z},$$

$$\frac{g_{\Xi\phi}}{g_{N\omega}} = -\frac{1 + \sqrt{6}z}{\sqrt{2} + \sqrt{3}z},$$

$$\frac{g_{N\phi}}{g_{N\omega}} = -\frac{\sqrt{6}z - 1}{\sqrt{2} + \sqrt{3}z}.$$

$$U_\Lambda(\rho_0) = -U_\Sigma(\rho_0) = -30 \text{ MeV}, U_\Xi(\rho_0) = -14 \text{ MeV}$$

Korea-China joint workshop for rare isotope physics



Letter

Correlation of the hyperon potential stiffness with hyperon constituents in neutron stars and heavy-ion collisions

Si-Na Wei ^{a, ID}, Zhao-Qing Feng ^{b, ID, *}, Wei-Zhou Jiang ^c

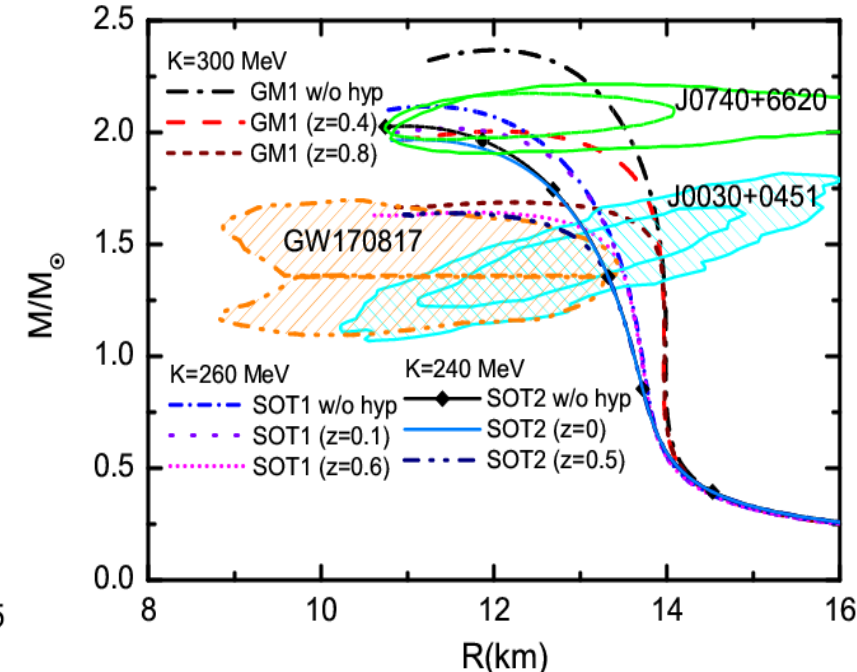
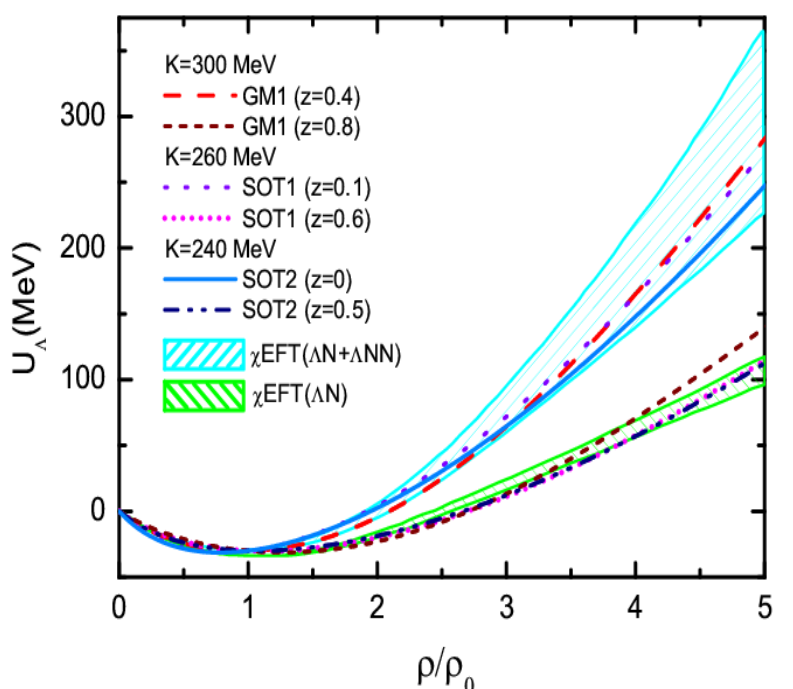
^a School of Mathematics and Physics, Guangxi Minzu University, Nanning 530006, China

^b School of Physics and Optoelectronics, South China University of Technology, Guangzhou 510640, China

^c School of Physics, Southeast University, Nanjing 211189, China

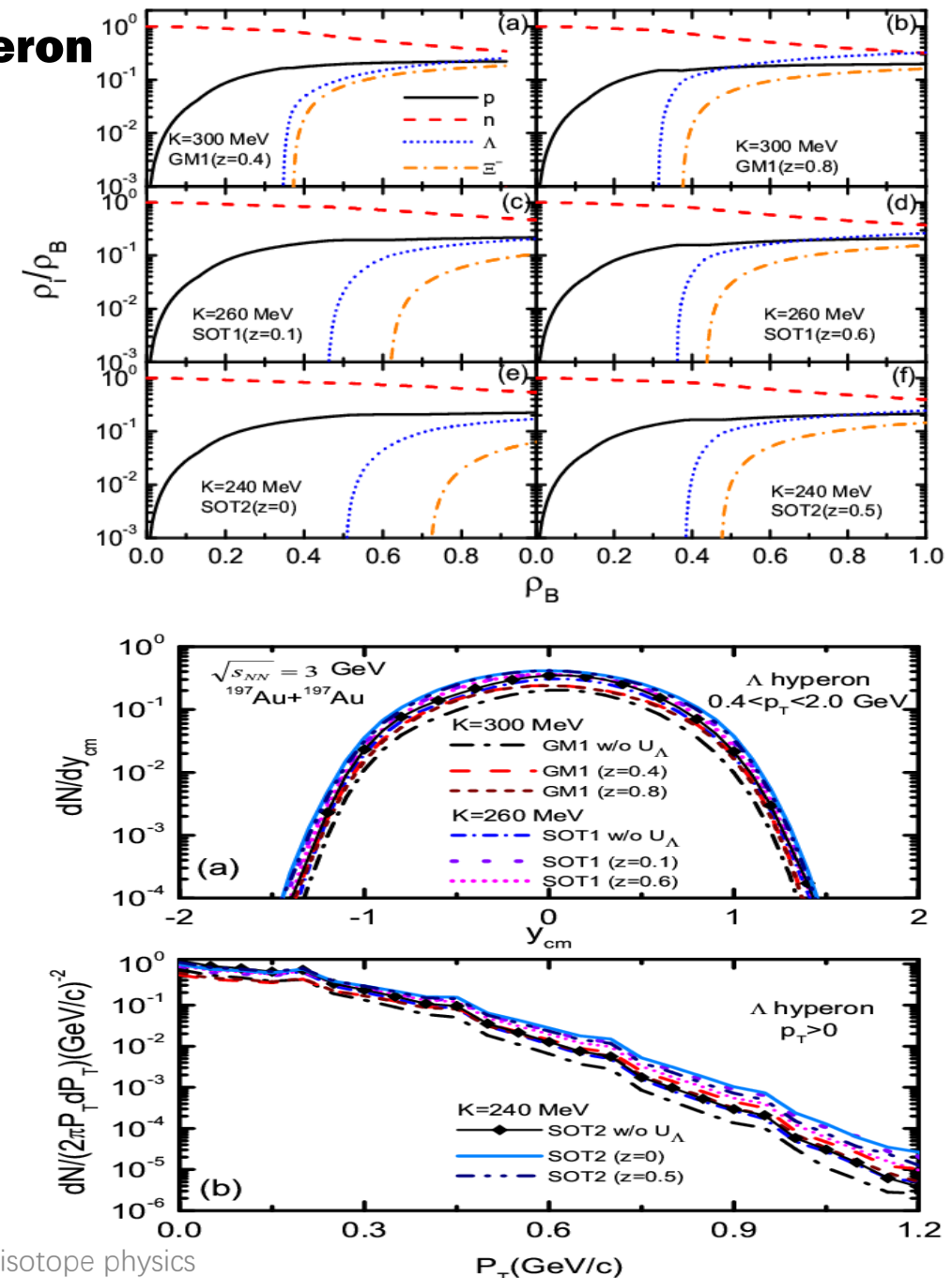
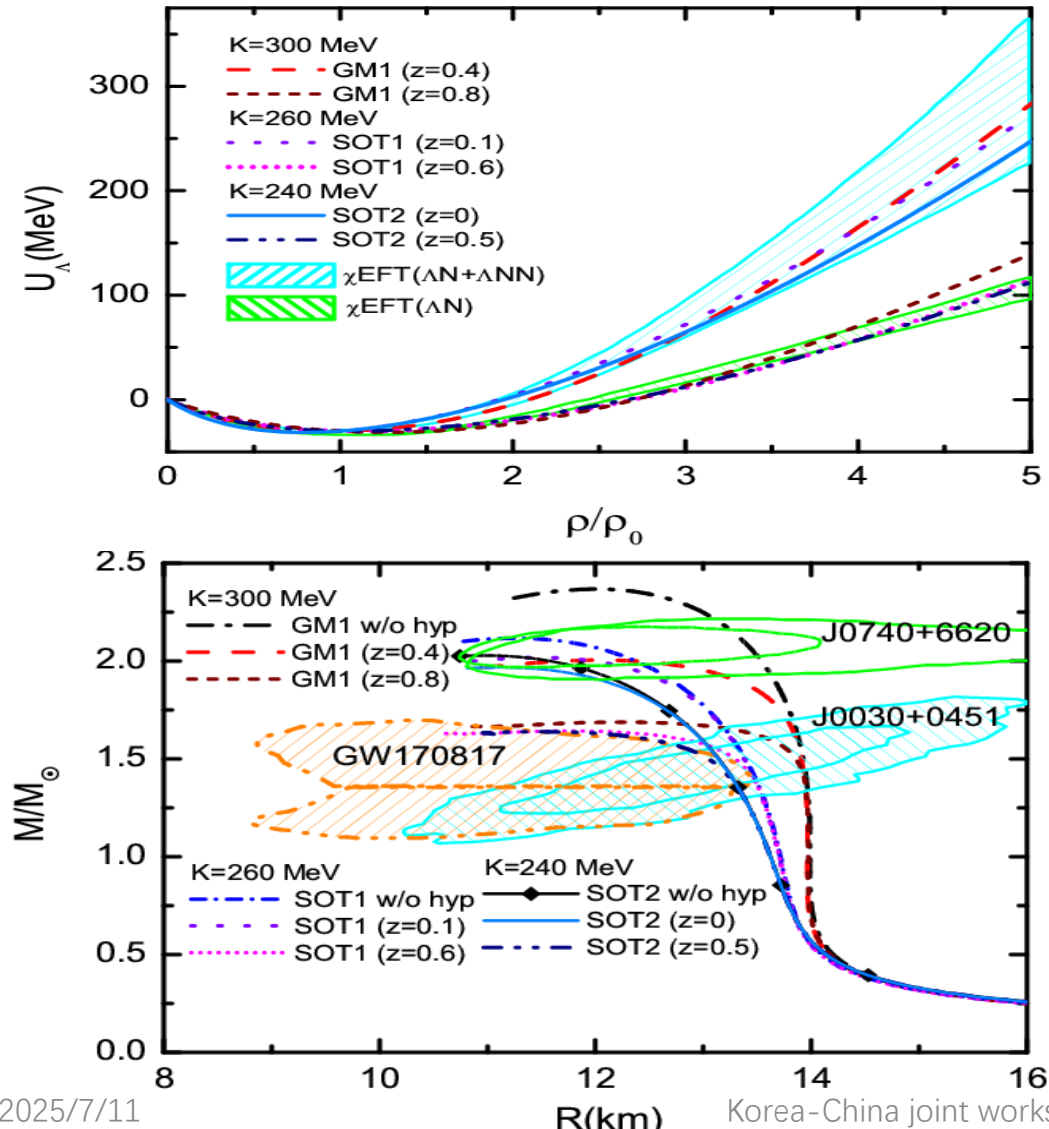
LQMD.RMF

Phys. Lett. B 853 (2024) 138658



Correlation of the hyperon potential stiffness with hyperon constituents in neutron stars and heavy-ion collisions

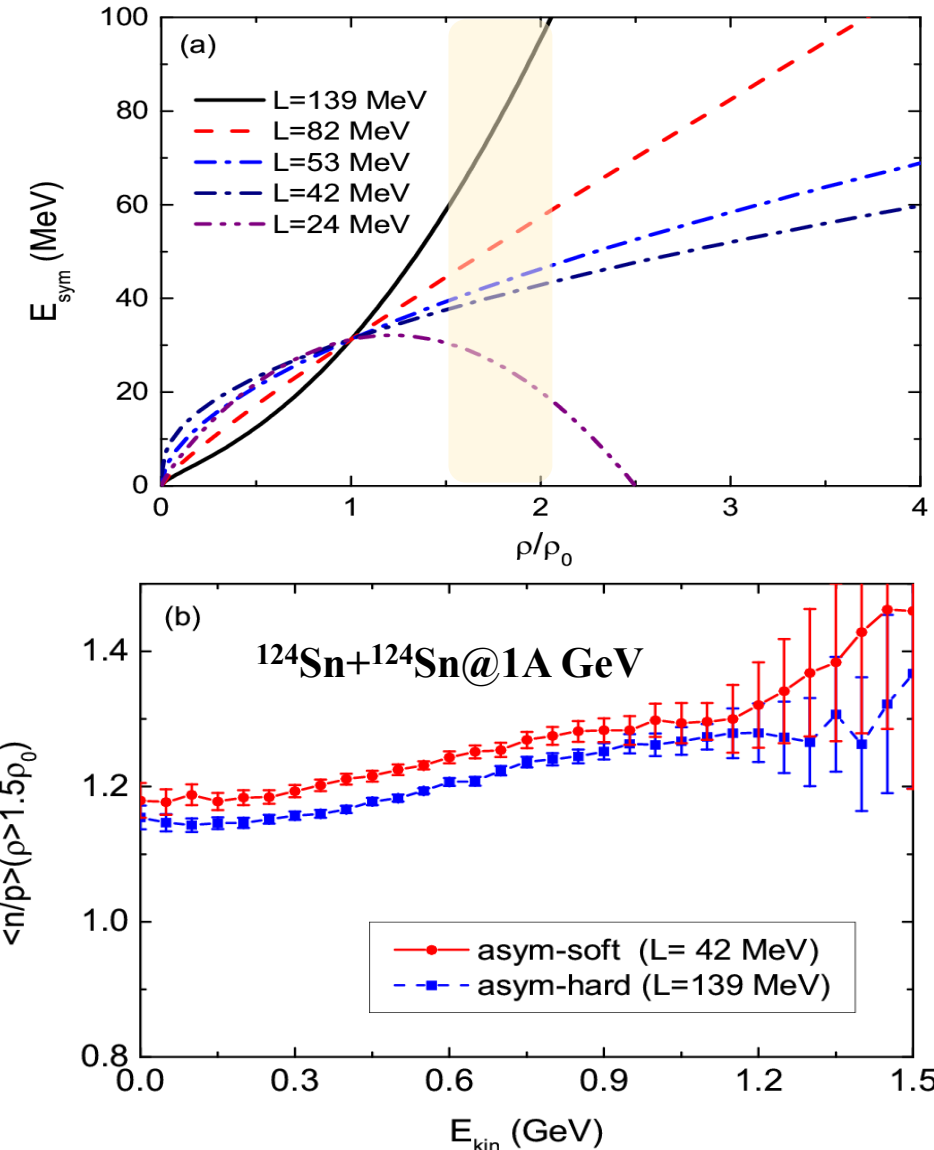
Si-Na Wei, ZQF, Wei-Zhou Jiang, PLB 853 (2024) 138658



Probing the high-density symmetry energy from subthreshold hyperon production in heavy-ion collisions

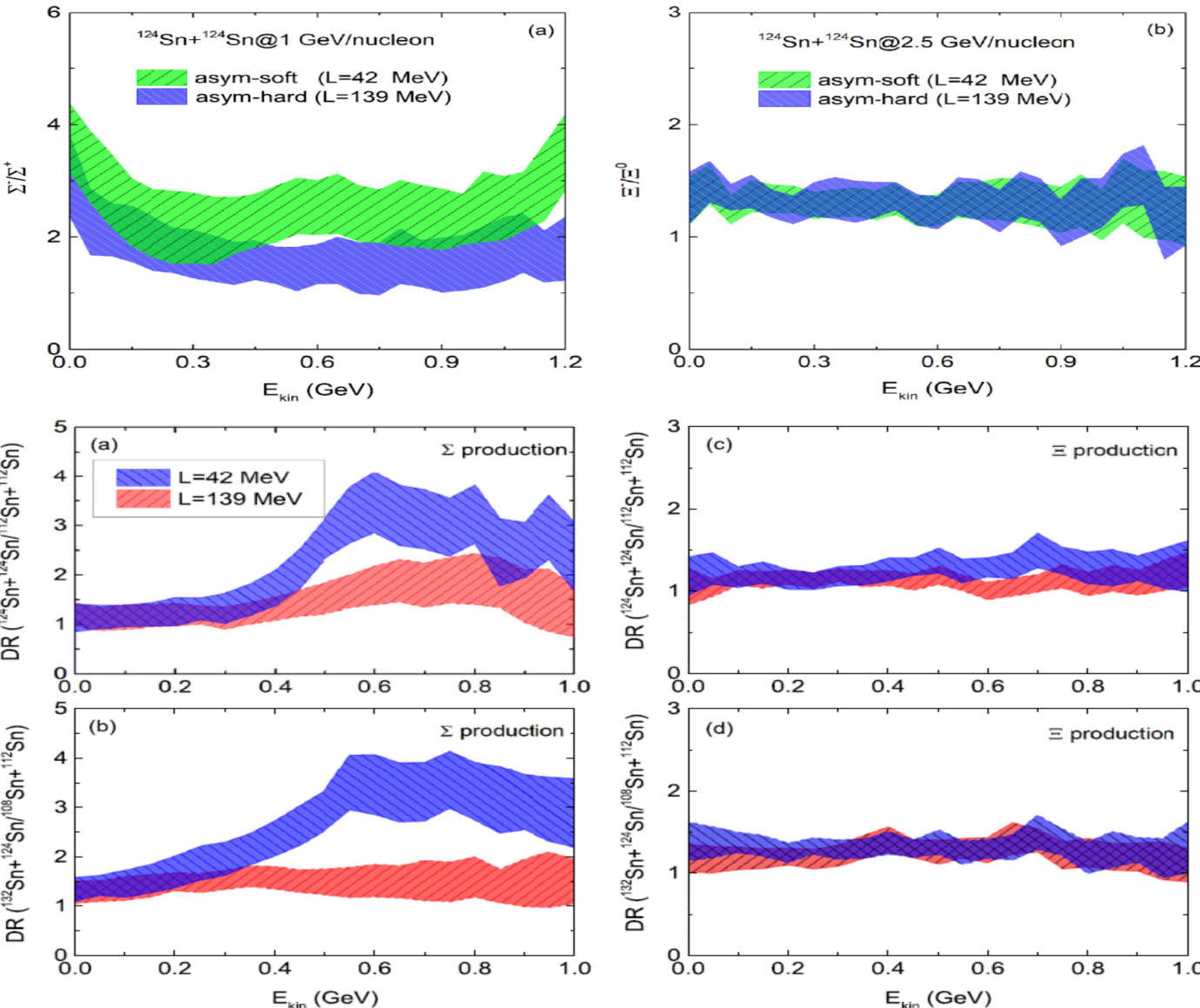
Zhao-Qing Feng

School of Physics and Optoelectronics, South China University of Technology, Guangzhou 510640, China



2025/7/11

High-density symmetry energy from hyperon production in heavy-ion collisions, Physics Letters B 846 (2023) 138180



Korea-China joint workshop for rare isotope physics

22

IV. Fragmentation reaction and hyperfragment production in HICs

Kinetic approach (动理学) for cluster production

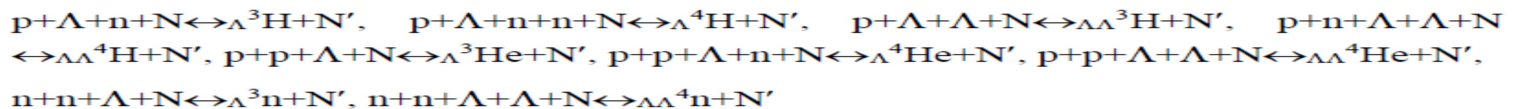
P. Danielewicz, G. F. Bertsch, Nuclear Physics A 533 (1991) 712-748

Akira Ono, Prog. Part. Nucl. Phys. 105, 139-179 (2019)

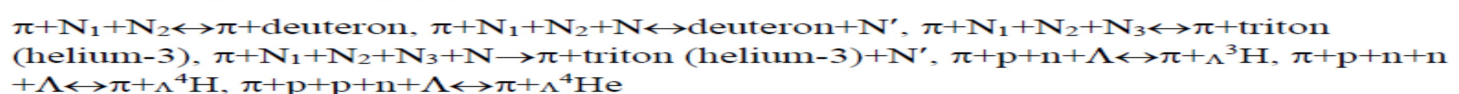
R. Wang, Y. G. Ma, L. W. Chen et al., Phys. Rev. C 108, L031601 (2023)

Hui-Gan Cheng, Zhao-Qing Feng, Phys. Rev. C 109, L021602 (2024)

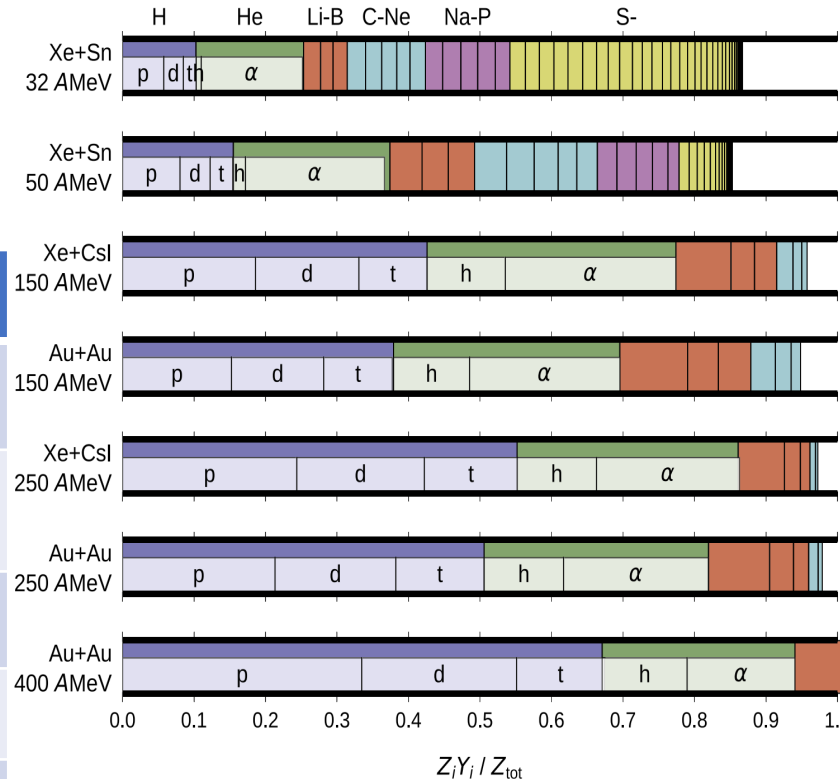
Year	models	Author(s)	Cluster(s)	Energy	Treatment(s)
1991	pBUU	P. Danielewicz et al.	<i>d, t, h</i>	fermi /intermediate energies	kinetic, Mott cut
2013	AMD-cluster	A. Ono	<i>2N, 3N, α</i>	fermi /intermediate energies	kinetic, fermionic mean field
2021	SMASH	J. Staudenmaier et al.	<i>d</i>	GeV and higher	kinetic
2022	PHQMD	G. Coci et al.	<i>d</i>	GeV and higher	kinetic
2023	LBUU	R. Wang et al.	<i>d, t, h, α</i>	intermediate energies	kinetic, Mott cut
2023	LQMD	H. G. Cheng and Z. Q. Feng	<i>d, t, h, α</i>	fermi /intermediate energies	Kinetic, binding energy, Pauli effects



以及π介子催化引起的反应道：

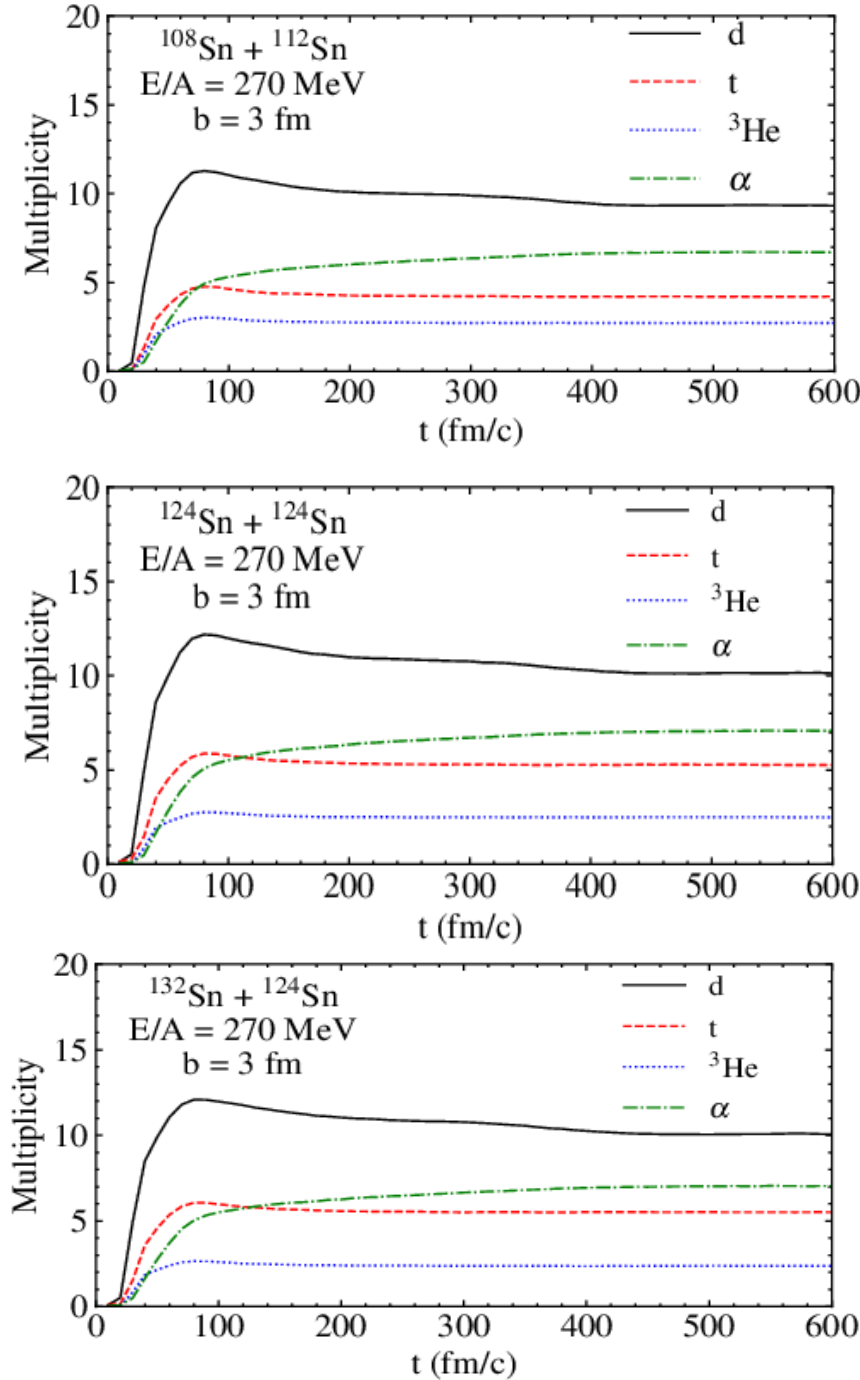


...

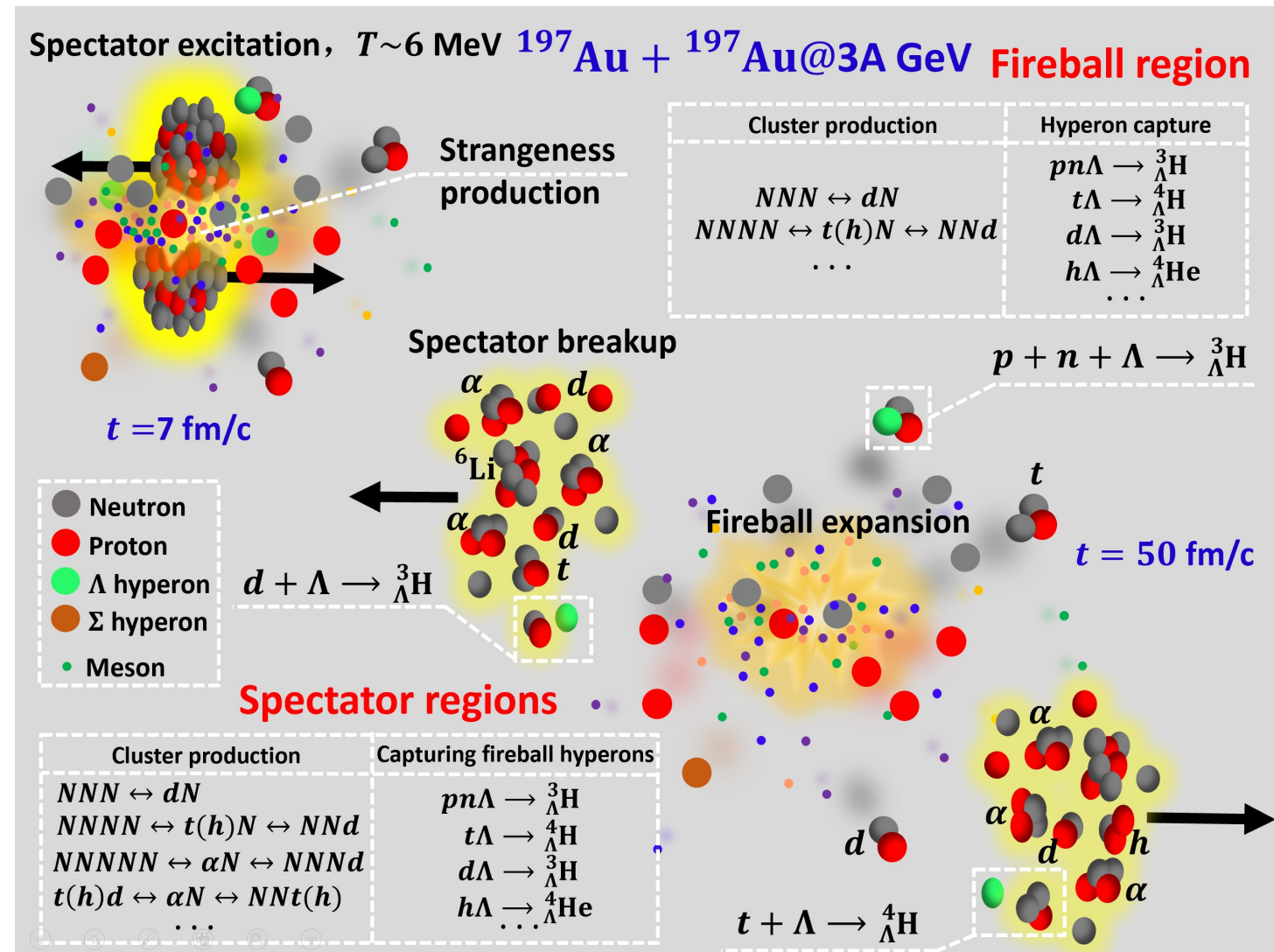


Clusters are produced by multinucleon or nucleon-cluster collisions

$$\frac{d\sigma}{d\Omega} = P(C_1 + C_2 \rightarrow C_3 + C_4) \times \frac{v_{\tilde{p}_{\text{rel}}}}{v} \frac{\left| [\partial e(k)/\partial k]_{k=\tilde{p}_{\text{rel}}} \right|}{\left| [\partial H(p_f)/\partial p_f]_{p_f=p_{\text{rel}}} \right|} \frac{p_{\text{rel}}^2}{\tilde{p}_{\text{rel}}^2} \left[\frac{d\sigma_{NN}}{d\Omega} \right]_{\tilde{p}_{\text{rel}}}$$



Schematic picture of nuclear cluster and hypercluster in HICs



Kinetic approach for cluster production (LQMD.cluster)

Novel approach to light-cluster production in heavy-ion collisions

Hui-Gan Cheng and Zhao-Qing Feng

School of Physics and Optoelectronics, South China University of Technology, Guangzhou 510640, China

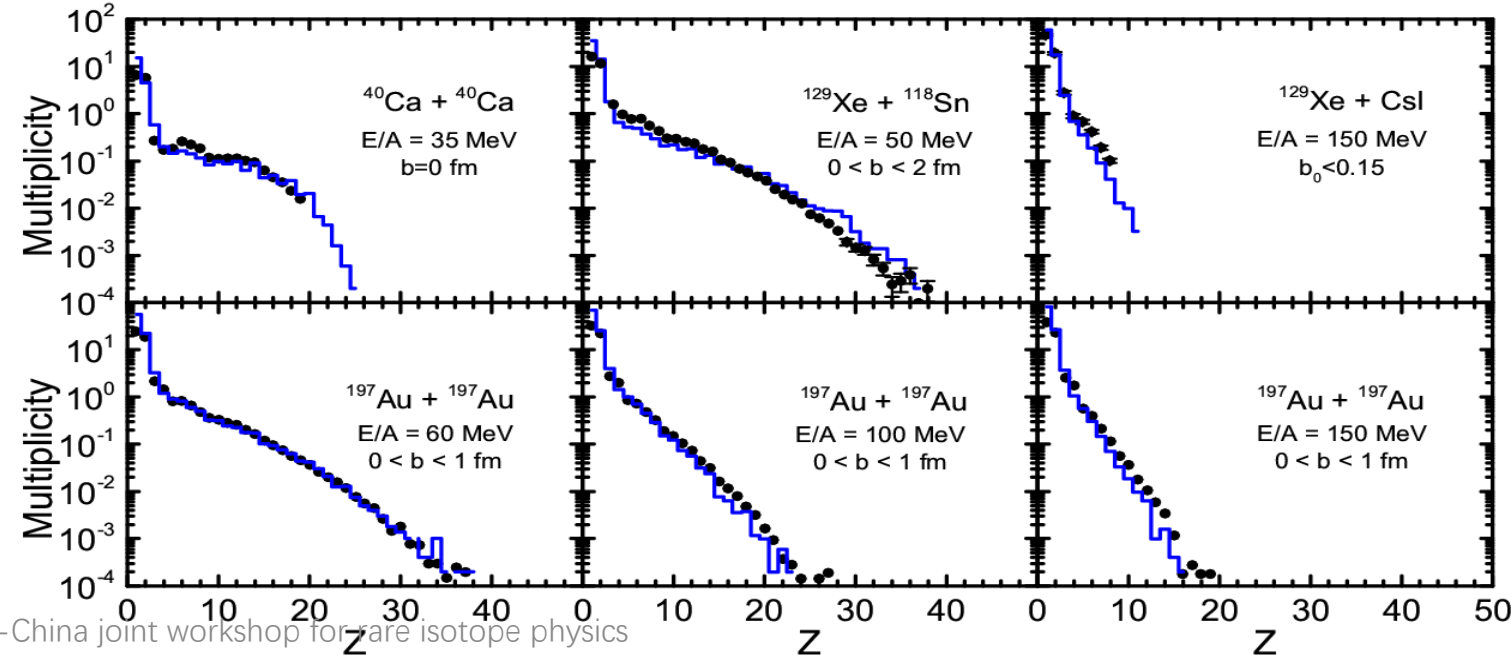
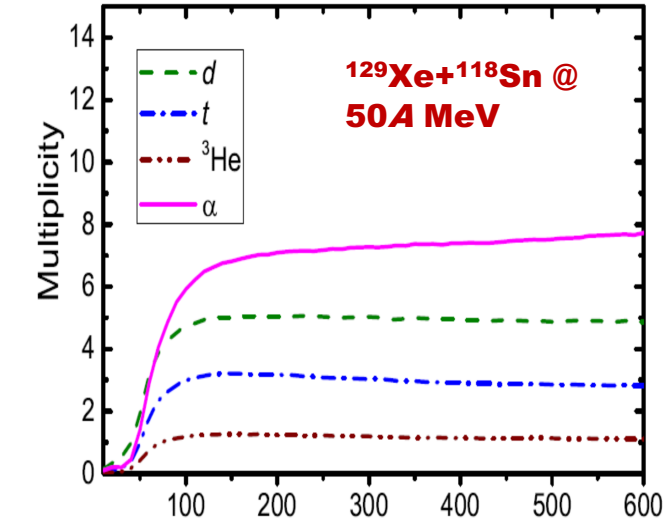
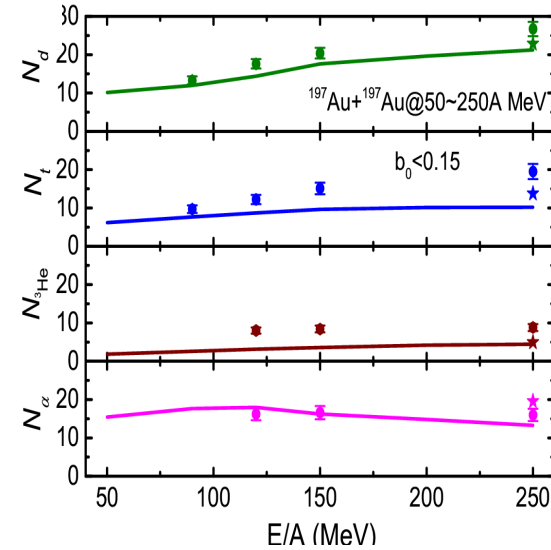
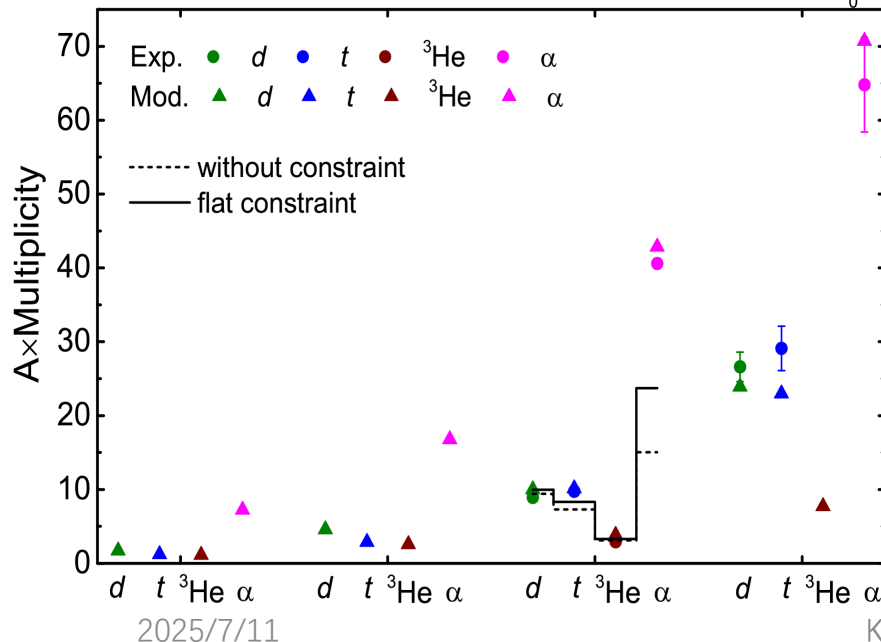
(Received 8 November 2023; accepted 25 January 2024; published 15 February 2024)

$$H = \sum_i \frac{\mathbf{p}_i^2}{2m} + \frac{\alpha}{2} \sum_{\substack{i,j \\ j \neq i}} \frac{\rho_{ij}}{\rho_0} + \frac{\beta}{1+\gamma} \sum_i \left(\sum_{j,j \neq i} \frac{\rho_{ij}}{\rho_0} \right)^\gamma$$

$$+ \frac{C_{sym}}{2} \sum_{\substack{i,j \\ j \neq i}} t_{z_i} t_{z_j} \frac{\rho_{ij}}{\rho_0} + \frac{g_{sur}}{2} \sum_{\substack{i,j \\ j \neq i}}' \left[\frac{3}{2L} - \left(\frac{\mathbf{r}_i - \mathbf{r}_j}{2L} \right)^2 \right] \frac{\rho_{ij}}{\rho_0}$$

$$+ \sum_i^{N_C} E_{z.p.}^i + \sum_i^{N_d} V_{corr} e^{-r_i^2/4L}$$

$^{16}\text{O} + ^{16}\text{O} @$ 50A MeV $^{40}\text{Ca} + ^{40}\text{Ca} @$ 50A MeV $^{129}\text{Xe} + ^{118}\text{Sn} @$ 50A MeV $b < 1\text{ fm}$ $^{197}\text{Au} + ^{197}\text{Au} @$ 90A MeV $b_0 < 0.15$

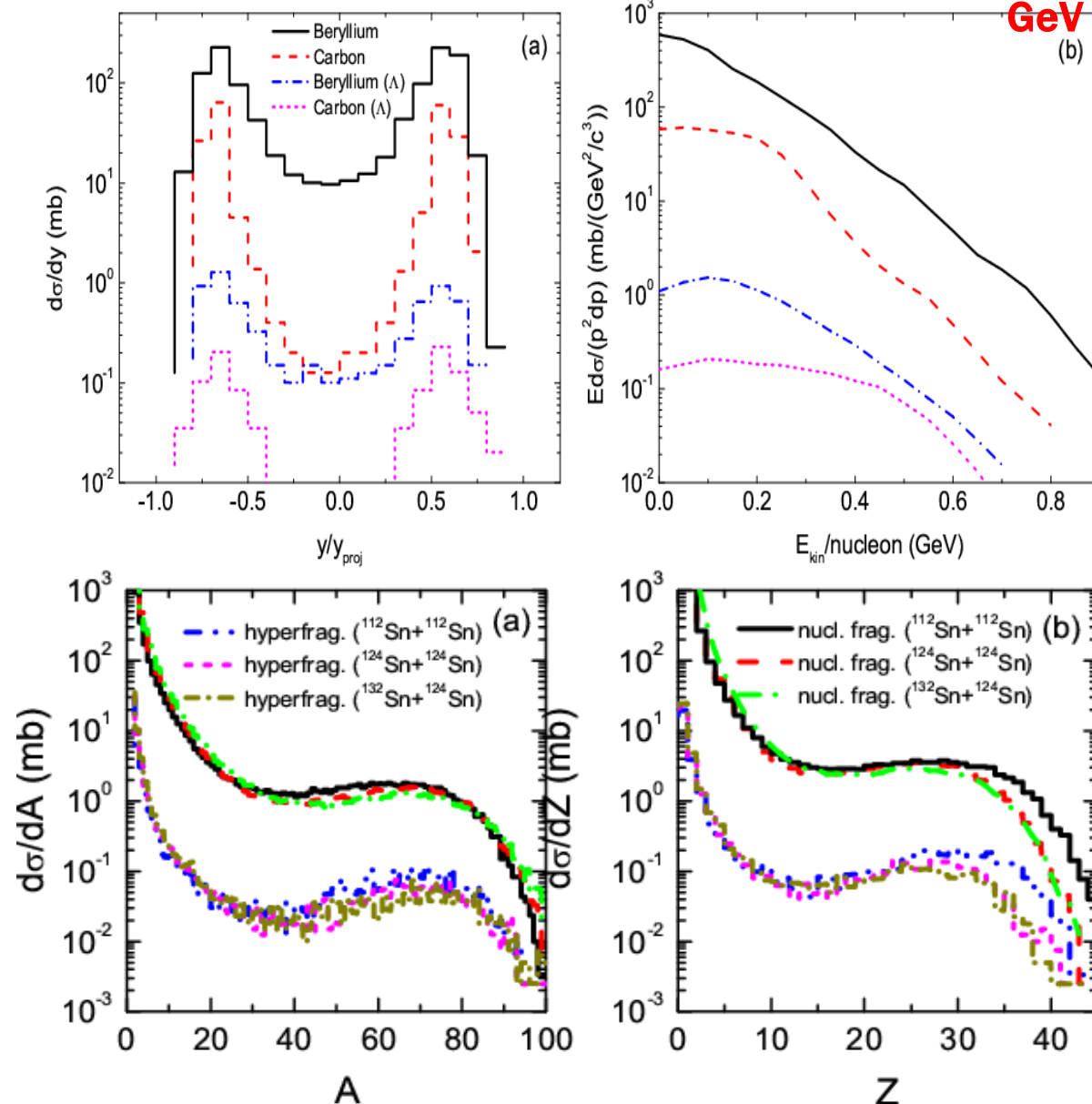
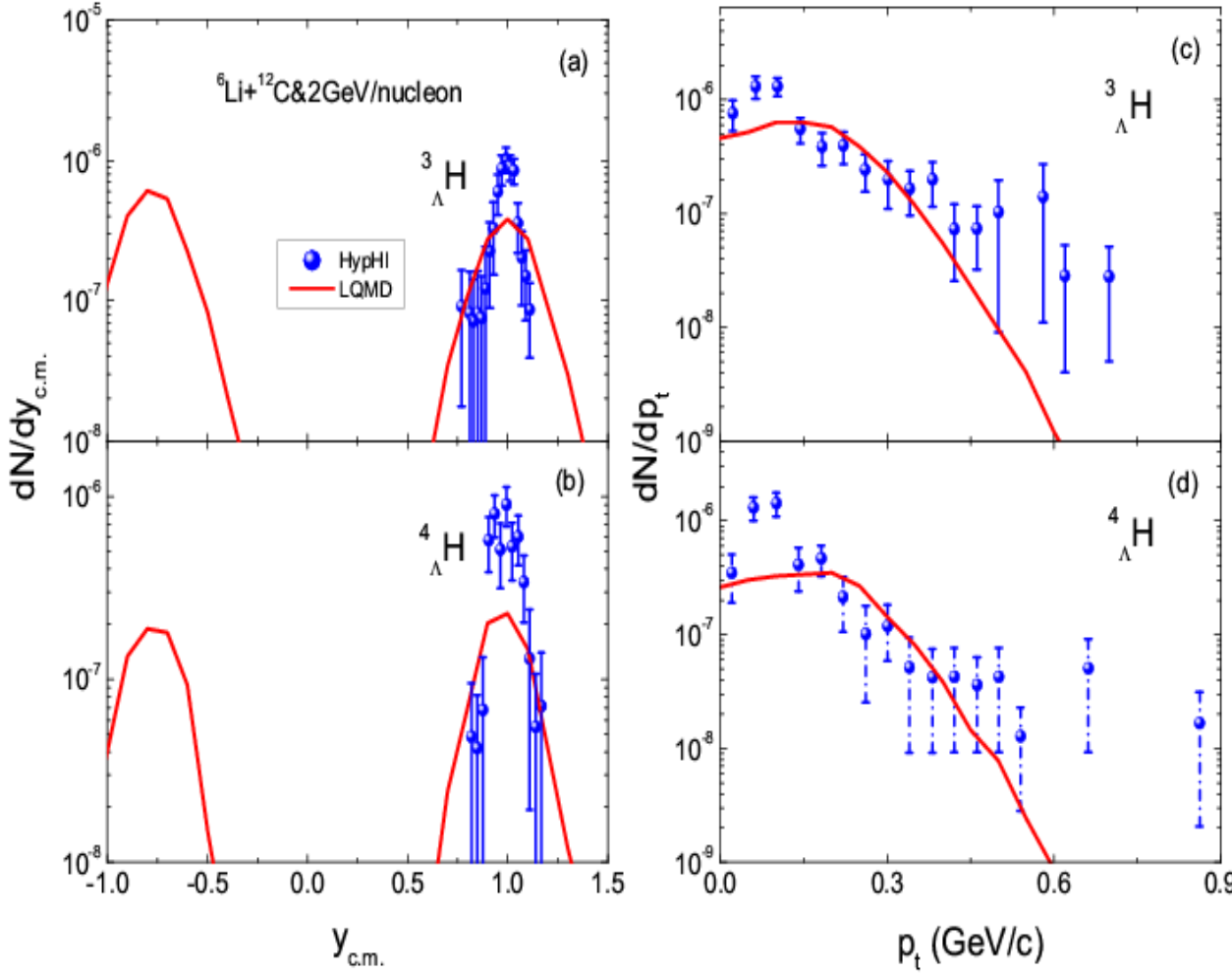


Hypernuclide production via HICs (Wigner density approach)

Z. Q. Feng, Phys. Rev. C 102, 044604 (2020)

Data: C. Rappold et al., (HypHI collaboration)

Phys. Lett. B 747, 129 (2015)



Multi-strangeness hypernuclide production

H.G. Cheng, Z. Q. Feng, Phys. Lett. B 824 (2022) 136849

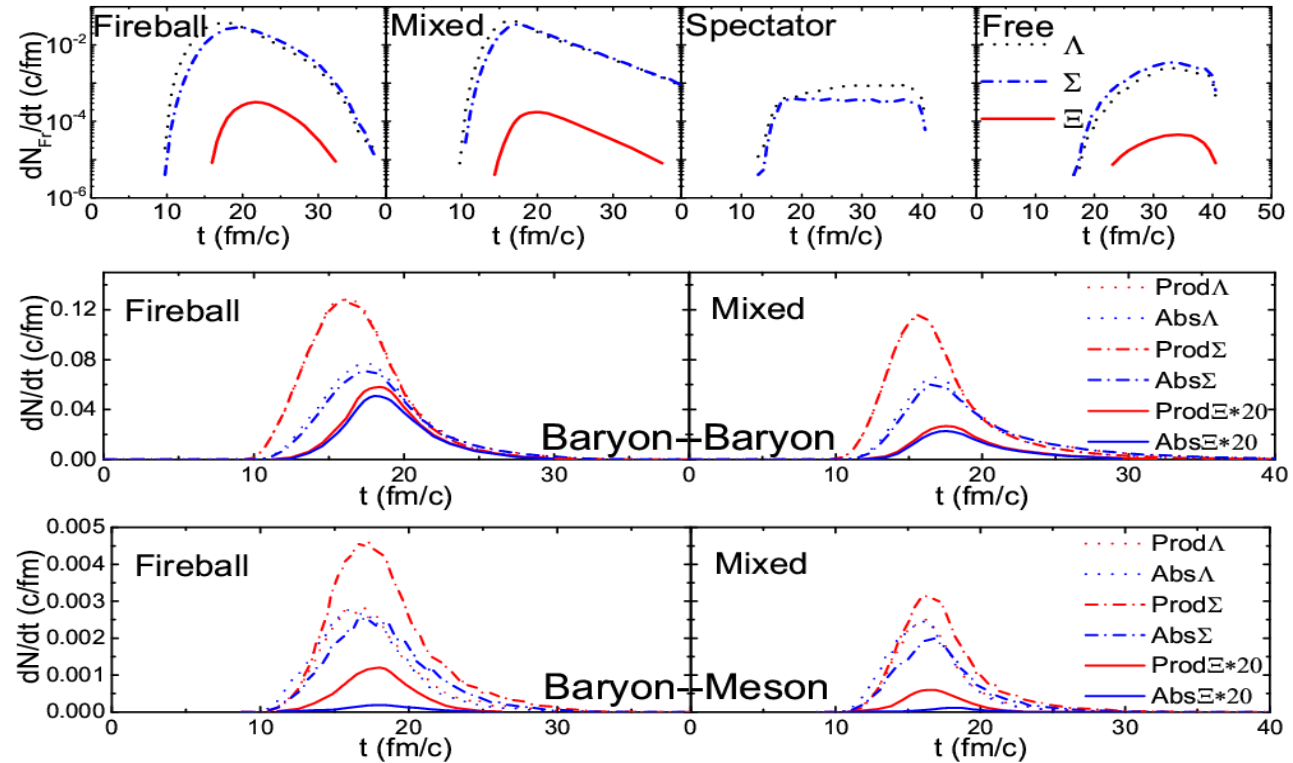
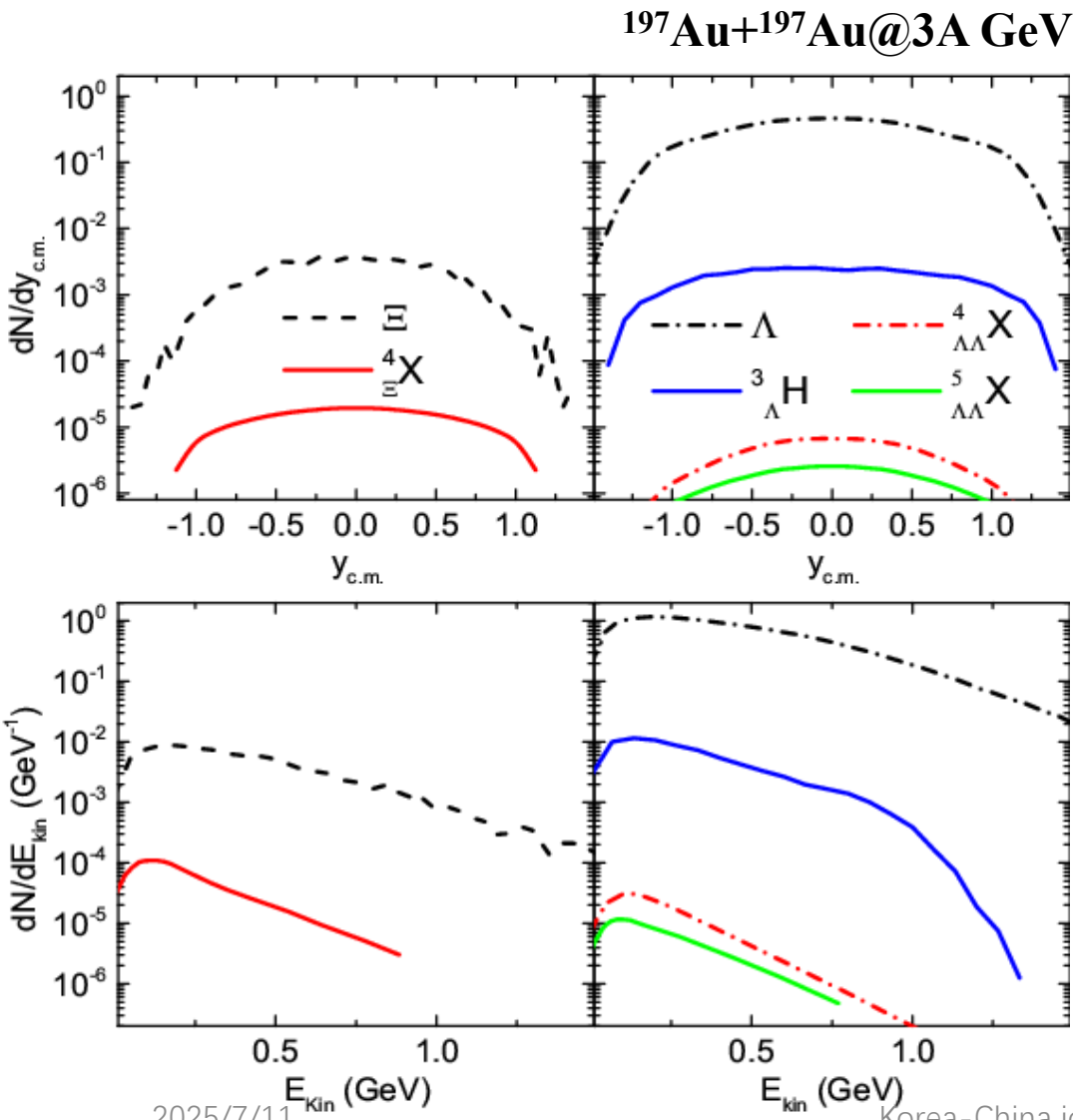


TABLE I. Comparison between cross sections of double lambda hypernuclei calculated with $r_0 = 3.5$ fm for Λ in $^{197}\text{Au} + ^{197}\text{Au}$ and $^{40}\text{Ca} + ^{40}\text{Ca}$ collisions at 3A GeV

Hypernuclei	Cross sections (mb)	
	$^{197}\text{Au} + ^{197}\text{Au}$	$^{40}\text{Ca} + ^{40}\text{Ca}$
$^4\Lambda\Lambda H$	2.6×10^{-2}	1.0×10^{-4}
$^4\Lambda\Lambda He$	1.0×10^{-2}	$\sim 10^{-5}$
$^5\Lambda\Lambda H$	5.9×10^{-3}	$\sim 10^{-5}$
$^5\Lambda\Lambda He$	5.1×10^{-3}	$\sim 10^{-5}$
$^5\Lambda\Lambda Li$	1.4×10^{-3}	$\sim 10^{-6}$
$^6\Lambda\Lambda He$	2.2×10^{-3}	$\sim 10^{-6}$
$^7\Lambda\Lambda He$	6.8×10^{-4}	$\lesssim 10^{-6}$

VI. Summary

- The high-density symmetry probes single and double ratios of Σ^-/Σ^+ (double ratio) via the isotopic reactions $^{112}\text{Sn}+^{112}\text{Sn}$ and $^{124}\text{Sn}+^{124}\text{Sn}$, in particular above 0.4 GeV.
- Hyperon production in heavy-ion collisions at HIAF energies provides a successful way for investigating the hyperon-nucleon potential in dense nuclear matter, e.g., $\Lambda\text{NN}, \Sigma\text{NN}, \Xi\text{NN}$ etc, might be constrained via heavy-ion collisions at HIAF.
- Kinetic approach is implemented in the LQMD transport model for the nuclear cluster production in Fermi energy heavy-ion collisions, hypercluster in the near future, in which the binding energy, multinucleon (cluster) collisions, Pauli principle, Mott effect etc are taken into account.

Thanks for your attention!